# FU JEN STUDIES

## NATURAL SCIENCES

NO. 12 1978

## CONTENTS



FU JEN UNIVERSITY

TAIPEI, TAIWAN, REPUBLIC OF CHINA

# THE CLOSED IDEALS OF SOME DIRICHLET ALGEBRAS

CHIN-SHIEN HU

It is known that the boundary value algebra $A_0$ on the unit circle $T$ is a Dirichlet algebra on $T$. Using singular maps $\phi$ on $T$, Browder and Wermer constructed[1] a class of Dirichlet subalgebras $A_0(\phi)$ of $A_0$. The closed ideals of $A_0(\phi)$ were characterized by Blumenthal[2]. In this paper, we consider some properties of $A_0(\phi)$. In section 1, we give a class of singular maps on $T$, and some examples of closed ideals of $A_0(\phi)$ by the result of Blumenthal. In section 2, we consider Möbius transformations $g$ which fix the unit circle $T$. We show that $A_0(g)$ contains only constant functions, if $g$ maps the interior of $T$ onto the exterior of $T$; and $A_0(g) = A_0$ if $g$ maps the interior of $T$ onto itself. At last, we also consider the isomorphisms of $A_0(\phi)$ induced by Möbius transformation $g$.

## 1. MAIN THEOREM AND EXAMPLES

Let $T$ be the unit circle $|z| = 1$ in the complex plane and $A_0$ the algebra of all continuous functions on $T$ which admit continuous extensions to $|z| \leqslant 1$, holomorphic on $|z| < 1$. Then $A_0$ is a Dirichlet algebra on $T$. Let $\phi$ be a homeomorphism of $T$ onto itself. We define

$$A_0(\phi) = \{f \in A_0 : f \circ \phi \in A_0\},$$

where $(f \circ \phi)(t) = (f(\phi))$. We call a homeomorphism $\phi$ of $T$ onto $T$ a "singular map" if it sends a subset of $T$ of Lebesgue measure 0 onto one of Lebesgue measure $2\pi$. Browder and Wermer[1] have proved the following theorem.

**Theorem A.** Let $\phi$ be a singular map on $T$. Then $A_0(\phi)$ is a proper Dirichlet subalgebra of $A_0$.

Now we construct some examples of singular maps of $T$, which are more general than that constructed by Leibowitz[3]. Let $I$ be the unit interval [0, 1] and $m$ the Lebesgue measure on $I$. Let $\phi_0$ be a monotone increasing continuous function from $I$ onto $I$, such that there exists a class of open intervals of $I$:

$$\{J_i : i = 1, 2, 3, \cdots\}$$

which satisfies the following conditions:

(i) $J_i \cap J_j = \Phi$ for $i \neq j$;

(ii) $\sum_{i=1}^{\infty} |J_i| = 1$, where $|J_i|$ is the length of $J_i$;

(iii) $\psi_0 | J_i =$ constant for each $i$.

There are many such functions. For example, the Lebesgue singular function[4] satisfies the above conditions. Put $I_n = [a_n, b_n]$ where $I_1 = [0, 1]$, $I_2 = [0, \frac{1}{2}]$, $I_3 = [\frac{1}{2}, 1]$, $I_4 = [0, \frac{1}{4}]$, $I_5 = [\frac{1}{4}, \frac{1}{2}]$, $I_6 = [\frac{1}{2}, \frac{3}{4}]$, $I_7 = [\frac{3}{4}, 1]$ etc, and let $\psi_n(t) = \psi_0\left(\frac{t - a_n}{b_n - a_n}\right)$ and $\psi = \sum_{n=1}^{\infty} \frac{\psi_n}{2^n}$. Then $\psi$ is a strictly increasing continuous function from $I$ onto $I$ such that $\psi' = 0$ almost everywhere.

By using the method of Leibowitz, we get the following theorem:

**Theorem 1.** The function $\phi$ defined by $\phi(e^{2\pi i t}) = e^{2\pi i \psi(t)}$ is a singular map on $T$, where $\psi$ is any function constructed as above.

From now on, let $\phi$ be a singular map on $T$. The closed ideals in the Dirichlet algebra $A_0(\phi)$ can be characterized as following (Blumenthal[2], Theorem 1).

**Theorem B.** $I$ is a closed ideal of $A_0(\phi)$ if and only if there exist closed ideals $J$, $K$ of $A_0$ such that

$$I = \{f \in A_0(\phi) : f \in J,\ f \circ \phi \in K\}.$$

We write $I = (J, K)_\phi$ if $I = \{f \in J : f \circ \phi \in K\}$. Now we give some examples of closed ideals in $A_0(\phi)$.

**Example 1.** Let $\alpha$ be a point in the unit disk $\{z : |z| \leqslant 1\}$. Put $J_\alpha = \{f \in A_0 : f(\alpha) = 0\}$. Then $J_\alpha$ is a maximal closed ideal of $A_0$. Let $I_\alpha = \{f \in A_0(\phi) : f(\alpha) = 0\}$. Then $I_\alpha = (J_\alpha, A_0)_\phi$ is a closed ideal in $A_0(\phi)$. In the case of $\alpha \in T$, we have another representation of $I_\alpha$.

**Example 2.** Let $K_\alpha = \{f \in A_0 : f(\phi^{-1}(\alpha)) = 0\}$. Then we have $I_\alpha = (J_\alpha, K_\alpha)_\phi = (J_\alpha, A_0)_\phi$ for each $|\alpha| = 1$.

From the above examples, we know that the above representation of closed ideals in $A_0(\phi)$ is not unique.

Each non-zero closed ideal in $A_0$ has the form $\psi I(S)$, where $I(S)$ is the ideal of all functions in $A_0$ which vanish on $S$. $S$ is a compact subset of $T$ with Lebesgue measure zero and $\psi$ is an inner function whose support on the circle is contained in $S$. Let $J = \psi_1 I(S_1)$ and $K = \psi_2 I(S_2)$. Then the closed ideals in $A_0(\phi)$ can also be written in the form:

$$I = (J, K)_\phi = \psi_1 I(S_1) \cap (\psi_2 \circ \phi^{-1})(I(S_1) \circ \phi^{-1}).$$

## 2. MÖBIUS TRANSFORMATIONS

Let $g$ be a Möbius transformation that maps the unit circle $T$ onto itself. Then $G$ is also a homeomorphism of $T$ onto itself. For $A_0(g)$ we have two different cases.

**Theorem 2.** If $g$ maps the exterior of $T$ onto the interior of $T$, then $A_0(g)$ consists of only constant functions.

*Proof.* Suppose that $f \in A_0(g)$, i.e. $f \in A_0$ and $f \circ g \in A_0$. Let $\tilde{f}$ and $\widetilde{f \circ g}$ be their holomorphic extensions to the unit disk, respectively. We define

$$h(z) = \begin{cases} \tilde{f}(g(z)) & \text{for } |z| \geqslant 1, \\ \widetilde{f \circ g}(z) & \text{for } |z| < 1. \end{cases}$$

Since $h(z) = (f \circ g)(z)$ for $|z| = 1$, $h$ is continuous on $|z| = 1$. Furthermore, $h$ is holomorphic for both $|z| > 1$ and $|z| < 1$. By Cauchy's Theorem, $h$ is holomorphic in the extended complex plane. Therefore $h$ is a constant function (Liouville's Theorem), so $f$ is constant on $T$. Hence $A_0(g)$ consists of only constant functions.

From this theorem, we know that in general $A_0(g)$ is not always a Dirichlet algebra.

**Theorem 3.** If $g$ maps the interior of $T$ onto itself, then $A_0(g) = A_0$.

*Proof.* For each $f \in A_0$, let $\tilde{f}$ be its holomorphic extension to the unit disk. We define

$$h(z) = \widetilde{(f \circ g)}(z) \quad \text{for } |z| \leqslant 1.$$

On the unit circle $T$ we have obviously $h(z) = (f \circ g)(z)$. Therefore $h$ is the holomorphic extension of $f \circ g$, i.e. $f \circ g \in A_0$. Hence $A_0 = A_0(g)$.

**Corollary.** $A_0(\phi \circ g) = A_0(\phi)$, where $g$ is a Möbius transformation as in Theorem 3, $\phi$ is a singular map of $T$.

*Proof.* $f \in A_0(\phi \circ g) \leftrightarrow f \in A_0$ and $f \circ \phi \circ g \in A_0$

$\leftrightarrow f \in A_0$ and $f \circ \phi \in A_0 \circ g^{-1} = A_0$

$\leftrightarrow f \in A_0(\phi)$.

From now on, let $g$ be a Möbius transformation as in Theorem 3, then the mapping $T_g : f \to f \circ g$ is an algebra automorphism of $A_0$ $(= A_0(g))$.

Hence $A_0 = A_0 \circ g = A_0(g)$. For the Dirichlet subalgebra $A_0(\phi)$ with respect to a singular map $\phi$ we have:

**Theorem 4.** $T_g$ is an isomorphism of $A_0(\phi)$ onto the Dirichlet algebra $A_0(g^{-1} \circ \phi)$.

*Proof.* First we show that $A_0(\phi) \circ g = A_0(g^{-1} \circ \phi)$:

$$\begin{aligned} h \in A_0(\phi) \circ g &\leftrightarrow h = f \circ g, \ f \in A_0 \text{ and } f \circ \phi \in A_0 \\ &\leftrightarrow h \in A_0 \text{ and } h \circ g^{-1} \circ \phi \in A_0 \\ &\leftrightarrow h \in A_0(g^{-1} \circ \phi). \end{aligned}$$

Since $\phi$ is singular and the Möbius transformation $g^{-1}$ maps sets of measure zero onto sets of measure zero, $g^{-1} \circ \phi$ is also singular. Thus $A_0(g^{-1} \circ \phi)$ is a Dirichlet subalgebra of $A_0$. Therefore $f \to f \circ g$ is an isomorphism of Dirichlet algebra $A_0(\phi)$ onto Dirichlet algebra $A_0(g^{-1} \circ \phi)$.

**Corollary.** Let $I = (J, K)_\phi$ be a closed ideal of $A_0(\phi)$. Then $I \circ g$ $(J \circ g, K)_{g^{-1} \circ \phi}$ is a closed ideal in $A_0(g^{-1} \circ \phi)$.

*Proof.*

$$\begin{aligned} I \circ g &= \{f \circ g : f \in J \text{ and } f \circ \phi \in K\} \\ &= \{h : h \circ g^{-1} \in J \text{ and } h \circ g^{-1} \circ \phi \in K\} \\ &= \{h : h \in J \circ g \text{ and } h \circ g^{-1} \circ \phi \in K\} \\ &= (J \circ g, K)_{g^{-1} \circ \phi}. \end{aligned}$$

Since $J \circ g$ and $K$ are closed ideals in $A_0$, $(J \circ g, K)_{g^{-1} \circ \phi}$ is a closed ideal in $A_0(g^{-1} \circ \phi)$.

## REFERENCES

(1) Browder, A. and J. Wermer, A method for constructing Dirichlet algebras, *Proc. Amer. Math. Soc., 15* (1964), 564-552.

(2) Blumenthal, R. G., The closed ideals of some Dirichlet and hypo-Dirichlet algebras, *Proc. Amer. Math. Soc., 32* (1972), 469-471.

(3) Leibowitz, G. M., *Lectures on Complex Function Algebras*, Scott, Foresman and Company, Glenview, 1970.

(4) Rudin, W., *Real and Complex Analysis*, McGraw-Hill, New York, 1966.

# NOTE ON ORIENTABLE RULED SURFACES IN $E^3$

YI-CHING YEN

## 1. INTRODUCTION

In his 1965 paper[1], T. J. Willmore proved that for an orientable closed surface $M$ in $E^3$ with mean curvature $H$, its total square mean curvature (or briefly called total mean curvature),

$$\int_M H^2 dM \geq 4\pi.$$

Equality holds if and only if $M$ is an Euclidean 2-sphere. Some results[2,3,4] have followed about the total mean curvatures of surfaces since then.

In this note we study the same problem on orientable ruled surfaces in $E^3$. We find that only conoids* have finite total mean curvatures, although it is known that the total Gaussian curvatures of ruled surfaces are constants for finite length of striction curves. We also get some other results subsequently. We shall prove the following:

**Theorem 1.** The conoid $M$ is the only orientable ruled surface in $E^3$ which has finite total mean curvature, and

$$\int_M H^2 dM \geqq \frac{1}{6L}\left(\ln \frac{p(L)}{p(0)}\right)^2,$$

where $L$ is the arc length of the director curve and $p$ is the distribution parameter of $M$.

**Theorem 2.** Let $u =$ constant be the generators and a family of asymptotic curves of a conoid. If an asymptotic curve, which is not a generator, has a vector representation $\vec{x}(u, v_0(u))$, then the family of asymptotic curves other than $u =$ constant takes the form

$$\vec{x}(u, v_0(u) + C\sqrt{|p(u)|}),$$

where $p$ is the distribution parameter of the surface and $C$ an arbitrary constant.

---

* These special surfaces have vector representations $\vec{x}(u, v)=(\int g(u)\cos u\, du + v\cos u, \int g(u)\sin u\, du + v\sin u, h(u))$, and according to James-James, "Mathematical Dictionary" we call them conoids.

**Corollary 1.** In a conoid, the distance of every generator cut by 2 asymptotic curves varies proportional to the square root of distribution parameter.

**Corollary 2.** In a conoid, the distances of every generator cut by the asymptotic curves are in constant ratios.

## 2. PRELIMINARIES

Let an orientable noncylindrical ruled surface have the vector representation

$$\vec{x}(u, v) = \sigma(u) + v\delta(u), \tag{1}$$

where $\sigma(u)$ is the striction curve and $\delta$ the director curve such that $\sigma' \cdot \delta' = 0$, and $\|\delta(u)\| = \|\delta'(u)\| = 1$. Then $u$ is the are length of $\delta$ and

$$\vec{x}_u = \sigma' + v\delta', \quad \vec{x}_v = \delta, \quad \vec{x}_u \times \vec{x}_v = (\sigma' + v\delta') \times \delta. \tag{2}$$

Let $\sigma' \times \delta = -p\delta'$, then we have $(\sigma', \delta', \delta) = p$, which is a function of $u$ and is called the distribution parameter.

$$\vec{x}_{uu} = \sigma'' + v\delta'', \quad \vec{x}_{uv} = \delta', \quad \vec{x}_{vv} = \vec{0}. \tag{3}$$

The coefficients of the 1st and 2nd fundamental form, the area element and the unit normal vector are obtained from (2) and (3) as

$$\left.\begin{aligned} &E = \sigma' \cdot \sigma' + v^2, \quad F = \sigma' \cdot \delta, \quad G = 1, \\ &EG - F^2 = p^2 + v^2, \quad \vec{U} = \frac{-p\delta' + v\delta' \times \delta}{(p^2 + v^2)^{1/2}}, \\ &\ell = \frac{1}{(p^2+v^2)^{1/2}}\,[rv^2 + p'v - p(\delta' \cdot \sigma'')], \quad m = \frac{-p}{(p^2+v^2)^{1/2}}, \quad n = 0, \end{aligned}\right\} \tag{4}$$

where $r = (\delta'', \delta', \delta)$.

Thus we have for the mean curvature $H$ of the surface

$$H = \frac{r(p^2 + v^2) + p'v + pa}{2(p^2 + v^2)^{3/2}}, \tag{5}$$

where $a = \sigma' \cdot \delta$ is a function of $u$.

**Proof of Theorem 1.** It is known that for the cylindrical ruled surface, its total mean curvature is infinity.

For a noncylindrical surface $M$, we take the parametrization such as (1), then the distribution parameter $p \neq 0$. Let the arc length of the director

curve be $L$.

If $r \neq 0$, then

$$\int_M H^2 dM = \int_0^L \int_{-\infty}^{\infty} \frac{(r(p^2+v^2)+p'v+pa)^2}{4(p^2+v^2)^{5/2}}\, dv\, du = \infty \tag{6}$$

If $r = 0$, then

$$\begin{aligned}\int_M H^2 dM &= \int_0^L \int_{-\infty}^{\infty} \frac{(p'v+pa)^2}{4(p^2+v^2)^{5/2}}\, dv\, du \\ &= \frac{1}{6}\int_0^L \frac{p'^2+2a^2}{p^2}\, du \qquad (7) \\ &\geqq \frac{1}{6}\int_0^L \frac{p'^2}{p^2}\, du \\ &\geqq \frac{1}{6L}\left(\int_0^L \frac{p'}{p}\, du\right)^2 \\ &= \frac{1}{6L}\left(\ln \frac{p(L)}{p(0)}\right)^2. \qquad (8)\end{aligned}$$

Equation (7) shows that $\int_M H^2 dM$ is constant.

Now we discuss what $r = 0$ means. Consider the position vector $\delta(u)$ drawn from origin 0, then $\delta$ forms a director cone on a unit sphere $\sum$ with center at 0. Since $\|\delta'(u)\| = 1$, $u$ is the arc length of the spherical curve $\delta$, hence its curvature vector $\delta'' \neq 0$. Also $\delta \cdot \delta' = \delta' \cdot \delta'' = 0$ shows that $\delta$ and $\delta''$ are perpendicular to $\delta'$. Thus $r = (\delta'', \delta', \delta) = 0$ (i. e. $\delta''$, $\delta'$, $\delta$ are coplanar) implies that $\delta'' = \lambda\delta$ with $\lambda \neq 0$, and $\lambda = -1$ in this case. Then $\delta$ is on a plane passing through 0, hence is a great circle of $\sum$. For brevity, we write

$$\delta(u) = (\cos u,\ \sin u,\ 0), \tag{9}$$

then

$$\delta'(u) = (-\sin u,\ \cos u,\ 0). \tag{10}$$

Since $\sigma' \cdot \delta' = 0$, $\sigma(u)$ can be expressed as

$$\sigma(u) = \left(\int g(u)\cos u\, du,\ \int g(u)\sin u\, du,\ h(u)\right). \tag{11}$$

Then $p(u) = (\sigma'(u), \delta'(u), \delta(u)) = -h'(u)$.

Thus, the ruled surface we obtain has an explicit form of (1) with $\delta$ and $\sigma$ as in (9) and (11). It has generators parallel to the $xy$-plane. It intersects the $z$-axis axis and $\sigma$. Hence, by definition, it is a conoid. Theorem 1 is thus proved.

**Proof of Theorem 2.** Applying $\ell$, $m$, and $n$ in (4), we have for the *DE.* of asymptotic curves of conoid

$$du((p'v + 2pf)\,du - 2pdv) = 0, \tag{12}$$

where $f = -\sigma'' \cdot \delta' / 2$, and is equal to $-\sigma' \cdot \delta / 2$ when $r = 0$. Therefore we have a family of asymptotic curves $u =$ constant and a family of curves having the *DE.*

$$\frac{dv}{du} - \frac{p'}{2p}v = f, \tag{13}$$

$f$ and $p$ are functions of $u$. Then

$$v = \sqrt{|p(u)|}\,(\int f(u) / \sqrt{|p(u)|}\,du + \bar{C}) = \lambda(u) + \bar{C}\sqrt{|p(u)|}. \tag{14}$$

Now an asymptotic curve $x(\vec{u}, v_0(u))$ with

$$v_0(u) = \lambda(u) + C_0\sqrt{|p(u)|}, \tag{15}$$

is obtained by assigning a constant value $C_0$ to $\bar{C}$ in (14).

Then the other asymptotic curves other than $u =$ constant take the form $\vec{x}(u, v(u))$ with

$$v(u) = \lambda(u) + \bar{C}\sqrt{|p(u)|} = v_0(u) + C\sqrt{|p(u)|}, \tag{16}$$

where $C = \bar{C} - C_0$ is an arbitary constant. q. e. d.

**Proof of Corollary 1.** Let the two asymptotic curves be $\vec{x}(u, v_k(u))$ with

$$v_k(u) = v_0(u) + C_k\sqrt{|p(u)|},\ k = i,\ j. \quad \text{Then}$$
$$v_i(u) - v_j(u) = (C_i - C_j)\sqrt{|p(u)|}.$$

Since $v_k$ are the directed distances of generators $u =$ constant from the striction curve, the distance $D_{ij}(u)$ on a generator cut by two asymptotic curves $\vec{x}(u, v_k(u))$, $k = i, j$, has the expression

$$D_{ij}(u) = |C_i - C_j|\sqrt{|p(u)|}. \tag{17}$$

Now fixed $i$, $j$ and change $u$, then the distances of the generators cut by the two asymptotic curves are proportional to $\sqrt{|p(u)|}$.

For the proof of Corollary 2, we take a constant value for $u$ and change the numbers of $i$, $j$, then the distances $D_{ij}$ are proportional to the constants

$|C_i - C_j|$, which are independent of the value of $u$, hence the asymptotic curves cut the generators in constant ratios.

## REFERENCES

(1) Willmore, T. J., Note on embedded surfaces, *An. Sti. Univ.* "Al. I. Cuza" Iasi. Seçt. I a Mat. 12 (1965) 493-496.

(2) Willmore, T. J., Mean curvature of immersed surfaces, *An. Sti. Univ.* "Al. I. Cuza" Iasi Seçt. I a Mat. 14 (1968) 99-103.

(3) Chen, B. Y., On the total curvature of immersed manifolds, I, II, III. *Amer. J. of Math.* **93** (1971) 148-162; ibid 95 (1973) 636-642.

(4) ———, Total mean curvature of immersed surface in $E^m$, *Trans. of the Amer. Math. Soc., Vol 218*, 1976, 333-341.

"Every good scientist should learn early that it is never in good taste to precisely designate the sum of two qnantities in the form:

$$\boxed{1 + 1 = 2.} \tag{1}$$

Anyone who has studied advanced mathematics is aware that $\ln e = 1$ and that also $\sin^2 x + \cos^2 x = 1$ and further $\sum_{n=0}^{\infty} \frac{1}{2^n} = 2$.

Therefore, Eq. (1) can be expressed more scientifically as:

$$\boxed{\ln e + (\sin^2 x + \cos^2 x) = \sum_{n=0}^{\infty} \frac{1}{2^n}.} \tag{2}$$

This can be further simplified by use of the relations:

$$1 = \cosh y \sqrt{1 - \tanh^2 y} \text{ and } e = \lim_{z \to \infty} \left(1 + \frac{1}{z}\right)^z$$

Equation (2) may therefore be rewritten as:

$$\boxed{\ln \left[\lim_{z \to \infty} \left(1 + \frac{1}{z}\right)^z\right] + (\sin^2 x + \cos^2 x) = \sum_{n=0}^{\infty} \frac{\cosh y \sqrt{1 - \tanh^2 y}}{2^n}} \tag{3}$$

At this point, it should be intuitively obvious that Eq. (3) is much clearer and more easily understood than Eq. (1).

Other methods of a similar nature can be used to further clarify Eq. (1), but these are left for the reader to discover once he grasps the underlying principles."

UNKNOWN BUT ASTUTE SOURCE

# A NEW MODEL OF ULTRASONIC ATTENUATION IN THE INTERMEDIATE STATE VERY NEAR $T_c$

FONG-JEN LIN

## ABSTRACT

A theoretical model is given to account for the observed oscillatory structure of ultrasonic wave absorption, $\alpha(T)$, in the intermediate state of Indium very close to the transition temperature $T_c$ ($T_c$-$T \lesssim 5$ mK). This model is based on the assumption that quasiparticles' free paths are much longer than the spacing of the "super lattice". Another important effect has also been found, which can be attributed to the quasiparticles with free paths comparable with the width of the normal region.

## INTRODUCTION

The density-of-state is modified from BCS due to quasiparticle scattering in the SNSN..."superlattice" in the intermediate state of a supercoductor.

These new features were found in transverse ultrasonic wave attenuation $\alpha_t(T)$ in Indium near $T_c$, the superconducting transition temperature. In Fig. 1 an oscillatory $\alpha_t(T)$ is seen for $\delta T = T_c - T \lesssim 5\ mK$ (millidegree $K$). In the range of interest in Fig. 1 the acoustic phonon energy $\hbar w$ is of order $0.01\ \Delta(T)$, the BCS[1] gap, and furthermore, $\hbar w$ is comparable with the band width and separation in the new quasiparticle energy spectrum just above $\Delta(T)$, so that the modified density-of-states can have a measurable effect on the observed $\alpha_t(T)$ due to electrons. The observed $\alpha_t(T)$ structure is found to be in good agreement with that determined from a theoretical model using the new quasiparticle density-of-states.

The intermediate state of a superconductor consists of periodic $NSNS...$ ($N$: normal, $S$: superconducting) regions. Therefore, ultrasonic attenuation is expected to be different from both pure superconducting and normal states. The theoretical model for intermediate state acoustic attenuation was given by Andreev and Bruk[2]. It takes into account the Joule heating due to $N$-$S$ wall motion, and has been in reasonable agreement with previous experimental studies[3,4]. However, our experimental condition is very different

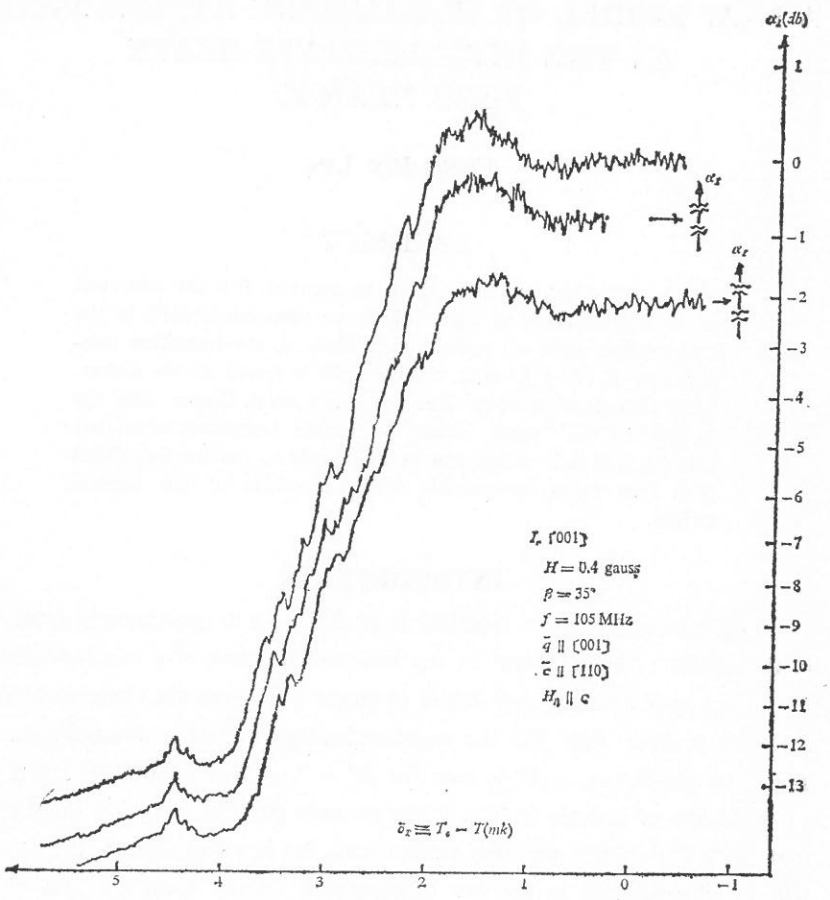


Fig. 1. Intermediate state attenuation versus $\delta T$ for 105 MHz transverse wave.

from previous experimental studies. Our whole intermediate state is in the temperature range very close to $T_c$. The value of $d_n/d$ ranges from 1 to 0.2 for $\delta T(\equiv T_c - T)$ of 0 to 5 $mK$. Here $d_n$ is the width of the normal lamina and $d$ is that of an $N$-$S$ pair. In this restricted temperature range, $\hbar w \gtrsim 0.01\,\Delta(T)$. To achieve this restricted condition a very small applied magnetic field $H < 1$ gauss is necessary.

The ultrasonic shear wave attenuation of Indium in the intermediate state was studied as a function of $\delta T$, where the range of $\delta T$ is of the order of 10 $mK$. In this small temperature interval the temperature was swept at

a rate of less than $3\,mK$ per minute with the sample directly immersed in liquid helium. The intermediate state was produced by the application of a slanting magnetic field of magnitude 0.4 gauss at a direction 35° from the sample surface. Transverse acoustic waves of frequency 105 MHz and 75 MHz had a propagation vector $\vec{q}$ perpendicular to the surface of the disk ((001) plane of Indium). The shear wave polarization vector $\vec{\varepsilon}$ was aligned in the [110] direction of Indium. The $N$-$S$ surfaces of the intermediate state were arranged either parallel or perpendicular to the direction of polarization of the shear wave. The features of Fig. 1 were consistently repeated, even to the relative positions on the $\delta T$ scale of the attenuation structure.

## THEORIES OF ULTRASONIC ATTENUATION IN THE INTERMEDIATE STATE

### (1) Geometrical Absorption

Treating the intermediate state as a combination of pure superconducting regions and pure normal regions, the absorption is determined entirely by the relative amount of normal and superconducting material sampled by the ultrasonic beam.

Case (a): Wave propagation vector $\vec{q}$ parallel to laminas (equivalent to parallel connection). Let $I_{oN(s)}$ be the initial intensity at $x = 0$ in the (superconducting) region and $I_{N(s)}$ be the attenuated intensity at distance $x$ in the normal (superconducting) region. Using the definition of attenuation $\alpha$, we have

$$I_N = I_{0N} \exp(-x\alpha_N),$$

and

$$I_S = I_{0S} \exp(-x\alpha_S).$$

For the parallel path case, therefore,

$$I_S + I_N = I_{0N} \exp(-x\alpha_N) + I_{0S} \exp(-x\alpha_S),$$

or

$$\frac{I_N + I_S}{I_{0N} + I_{0S}} = \frac{I_{0N}}{I_{0N} + I_{0S}} \exp(-x\alpha_N) + \frac{I_{0S}}{I_{0N} + I_{0S}} \exp(-x\alpha_S),$$

$$= \frac{I_S}{I_{0I}} = \exp(-\alpha_I x).$$

Hence

$$\exp(-x\alpha_I) = \rho_N \exp(-\alpha_N) + \rho_S \exp(-x\alpha_S), \tag{1}$$

where

$$\rho_N = \text{fraction of normal region}$$

$$= \frac{I_{0N}}{I_{0N} + I_{0S}}$$

and

$$\rho_S = \text{fraction of superconducting region}$$

$$= \frac{I_{0S}}{I_{0N} + I_{0S}}.$$

Case (b): Wave propagation vector $\vec{q}$ perpendicular to laminas ($N$-$S$ connected in series). For this case we have

$$I_0 \exp(-\alpha_I x) = I_0 \exp(-\alpha_N x_N) \exp(-\alpha_S x_S)$$

so that

$$-\alpha_I x = -\alpha_N x \alpha_N - \alpha_S x_S$$

$$\alpha_I = \rho_N \alpha_N + \rho_S \alpha_S. \tag{2}$$

**(2) Absorption due to Boundary Wall Motion.**

The equlibrium magnetic field at normal side of the laminars $S$-$N$ interfaces is equal to $H_c$. $H_c$ is a function of pressure and temperature, and since the passage of the acoustic wave causes these to change, the magnetic field at the interfaces fails to be $H_c$. Since this violates the equilibrium condition, the boundary between phases moves. Hence, an $AC$ magnetic field appears, eddy currents are induced, and energy is lost through Joule heating. The attenuation obtained by Andreev and Bruk[2,5] is

$$\alpha = \frac{4[A + 1 - (\vec{m} \cdot \vec{n})^2]^2}{\rho\sigma(d_N + d_S)S_l^3\delta} \left(\frac{cH_c}{8\pi}\right)^2, \tag{3}$$

under the conditions

$$\lambda_S \gg \delta,\ d_N,$$

$$d_N \gg \delta \tag{4}$$

where

$$A = -\frac{\rho}{H_{co}}\left(S_l^2 - S_t^2\right)\left[\left(\frac{\partial H_c}{\partial P}\right)_T - \left(\frac{\partial H_c}{\partial T}\right)_P \frac{T}{\rho c}\left(\frac{\partial \rho}{\partial T}\right)_P\right]. \qquad (5)$$

In equations (3) to (5) $\rho$ is the density; $s_1$ and $s_t$ are the longitudinal and transverse sound velocities; $H_{co}$ is the critical field at the equilibrium temperature $T$ and pressure $P$; $\vec{m}$, $\vec{n}$ are the unit vectors in the direction of the magnetic field and the sound propagation vector; $\sigma$ is the normal conductivity; $\delta$ is the normal metal skin depth given by

$$\delta = \frac{c}{(2\pi\sigma w)^{1/2}}.$$

In equation (3), it is assumed that the sound wave length $\lambda_S \gg d_N$. Thus the mechanism is important only for much lower sound frequencies than used in the present experiments, where $\lambda \simeq 10^{-3}$ cm and $d_n > 10^{-2}$ cm. In any case the Joule heating attenuation predicted by Andreev has none of the features observed near $T_c$ in the present work. (See references 3 and 4, in which the Andreev Joule heating absorption is examined experimentally).

**(3) Absorption due to Electrons orbiting in A Magnetic Field[5].**

We summarize the results as follows:

(a) The Larmor radius $R$ is much larger than the mean free path of electron, $l$.

(i) $\lambda_S \ll d_N$,

$$\frac{\alpha_I}{\alpha_N} = \rho_N. \qquad (6)$$

(ii) $\lambda_S \gg d_N$,

$$\frac{\alpha_I}{\alpha_N} = \text{const. } \rho_N \frac{d_N}{\lambda_S} \qquad (7)$$

(b) $R \ll l$,

$$\alpha_I = \alpha_0 + \Delta\alpha \qquad (8)$$

$\alpha_0$ is the monotonic part

$$\alpha_0 = \rho_N \Phi(2d_N/\lambda_S)\, \alpha_0^N(H)$$

where $\Phi(x)$ varies from 0 to 1, $\alpha_0^N(H)$ is the field dependent attenuation of normal state, and $\Delta\alpha$ is the oscillatory part, smaller than $\alpha_0$ by a factor $(R/d)^{1/2}$.

In our experiment the electron mean-free-path $l$ is of order 0.1 cm, $R$

is of order 1 cm, and $\lambda_S \ll d_N$. In other words our experiment is in catagory (a) (i). Thus,

$$\alpha_I = \rho_N \alpha_N$$

This means that the attenuation in the intermediate state is the same as in the normal state. Therefore nothing new is predicted from a consideration of the orbiting of electrons.

**(4) Absorption due to Quasiparticle Relaxation.**

This is a model for a peak in $\alpha_t$ near $T_c$[6] requiring boundary motion. The peak, which was found to be amplitude dependent and to increase in magnitude very markedly with frequency, is attributed to quasiparticle relaxation. However it appears that the phenomena of interest in the present work are a separate effect. A series of peaks is found near $T_c$ which give strong indication of being concerned with quasiparticle scattering from boundaries.

## NEW MODEL OF ULTRASONIC ATTENUATION

**(1) Ultrasonic Attention due to Quasiparticles with Free Paths Much Longer Than Spacing of "Superlattice", *d*.**

The theories existing so far can not explain our experimental result because they fail to recognize the periodic *N-S* laminas as a whole. Since in the intermediate state there is a periodic array consisting of alternating normal and superconducting laminas, it is not correct to investigate quasiparticle properties separately either in the normal or in superconducting region. In other words, neither the normal nor the superconducting region in the intermediate state is equivalent to the pure normal or superconducting state, because the electrons see the *N-S* laminar structure as a whole.

In our Indium sample in the liquid helium temperature range, the mean free path of electrons is of the order of 0.1 cm and our laminar spacing $d(\equiv d_s + d_n)$ is also of the order of 0.1 cm. Hence a significant fraction of the total number of electrons in the effective zone has free paths larger than the laminar spacing $d$. Therefore it is essential to treat the periodic array of *N-S* laminas as a whole. When this is done we expect to find the new energy spectrum to be different from that for both pure super-

conducting or the normal state, and an entirely new density of energy states will result. In turn this new density-of-state is expected to lead to new features of the attenuation, which are not observed when the BCS density of states is used.

The problem of the energy spectrum of the intermediate state is equivalent to the energy spectrum of excitations associated with a one dimensional step potential. We are faced to solve the Bogolubov equation of "electron-hole" coupled excitation. Van Gelder[7] has made a calculation of the energy spectum of "electron-hole" coupled excitation and found the following solution for the simplified one dimensional Bogolubov equation

$$\begin{bmatrix} \left(\frac{P^3}{2m} - \frac{\hbar^2 k_x^2}{2m}\right) & \Delta(x, T) \\ \Delta(x, T) & -\left(\frac{P^2}{2m} - \frac{\hbar^2 k_x^2}{2m}\right) \end{bmatrix} \begin{bmatrix} u(x) \\ v(x) \end{bmatrix} = E \begin{bmatrix} u(x) \\ v(x) \end{bmatrix} \tag{9}$$

where $\Delta(x, T)$ is the pair potential or energy gap in the superconductor, such that

$$\Delta(x, T) = \Delta(T) \text{ in the superconducting region,}$$

and

$$\Delta(x, T) = 0 \text{ in the normal region.} \tag{10}$$

Here $[u/v]$ is the two component wave function of the "electron-hole" paired excitation with eigenvalue $E$, subject to to the normalization condition

$$u^2 + v^2 = 1 \tag{11}$$

There are two special cases:

$$u = 1,\ v = 0 \text{ for } E > 0 \text{ (electron-like); and}$$
$$u = 0,\ v = 1 \text{ for } E < 0 \text{ (hole-like).}$$

Setting

$$\varepsilon = E/\Delta \tag{12}$$

we have the solution for $\varepsilon > 1$

$$\cos[K - k_x)d] = \cos(A\varepsilon)\cos[B(\varepsilon^2 - 1)^{1/2}] - \left[\frac{\varepsilon}{(\varepsilon^2 - 1)^{1/2}}\right]\sin(A\varepsilon)\sin[B(1 - \varepsilon^2)^{1/2}] \tag{13}$$

and for $\varepsilon < 1$

$$\cos[K - k_x)d] = \cos(A\varepsilon)\cosh[1 - \varepsilon^2)^{1/2}] - \left[\frac{\varepsilon}{(1 - \varepsilon^2)^{1/2}}\right]\sin(A\varepsilon)\sinh[B(1 - \varepsilon^2)^{1/2}]. \tag{14}$$

$K$ is the Bloch momentum along the $x$-axis (i. e. normal to the laminas), $k_x$ is given by

$$k_F^2 = k_x^2 + k_y^2 + k_z^2 \tag{15}$$

and

$$A = d_N/\alpha$$
$$B = d_S/\alpha$$
$$\alpha = \hbar^2 k_x/m\Delta$$

Writing equations (13) and (14) symbolically as

$$F(K) = F(\varepsilon)$$

the range of value of $K$ is

$$-1 \leq F(K) \leq 1$$

Therefore, the allowed energies are such as to confine $F(\varepsilon)$ in the region

$$-1 \leq F(\varepsilon) \leq 1$$

In other words, $\varepsilon$ values such that $|F(\varepsilon)| > 1$ are forbidden.

The density of state in the forbidden region is zero, in the allowed region, it is given by

$$\rho(\varepsilon) = \frac{\hbar v_F}{\sqrt{3}\,\Delta}\frac{dk}{d\varepsilon}. \tag{16}$$

From numerical solutions, the allowed band width and band separation are of the order of $0.01\,\Delta(T)$. The allowed energies below the gap $\Delta(T)$ are narrow and rather widely separated lines, the spacing between lines being of order $0.1\,\Delta(T)$.

The transverse wave attenuation $\alpha_t$ by electrons in Indium near $T_c$ when $ql > 1$, as in the present case, is given by $\alpha_t = \alpha_{tE} + \alpha_{tD}$ where $\alpha_{tE}$ is the contribution from electromagnetic interaction, and $\alpha_{tD}$ is arising from shear deformation of the Fermi surface. At temperatures very close to $T_c$,

both $\alpha_t$ and the variation of $\alpha_t$ are dominated by electromagnetic interaction. Therefore, we shall consider only attenation due to electromagnetic interaction. The ratio of $\alpha_I$ (attenuation in the modified $N$ or $S$ region of the intermediate state) to $\alpha_N$ (attenuation in the normal state) is[8]:

$$\frac{\alpha_I}{\alpha_N} = \frac{\sigma_{1I}/\sigma_{1N}(\gamma^2+1)}{(\gamma+\sigma_{2I}/\sigma_{1N})^2+(\sigma_{1I}/\sigma_{1N})^2} \tag{17}$$

where

$$\gamma = \frac{q^2c^2}{4\pi w\,\sigma_{1N}}$$

$\sigma_1$ and $\sigma_2$ are the real and imaginary part of conductivity $\sigma$, $\sigma_{2I}/\sigma_{1N}$ is only important for the case that the density of states of a quasiparticle follow the BCS density of states, $\gamma$ is of order of $10^{-2}$. For the first approximation

$$\frac{\alpha_I}{\alpha_N} \simeq \frac{1}{(\sigma_{1I}/\sigma_{1N})}$$

The expression for $(\sigma_{1I}/\sigma_{1N})$ appropriate to the electromagnetic absorption is given by Mattis and Bardeen[9]:
in a modified super conducting region

$$\left(\frac{\sigma_{1S'}}{\sigma_{1N}}\right)_+ = \frac{2}{(\hbar w/\Delta)}\int_1^\infty \rho(\varepsilon)\rho\left(\varepsilon+\frac{\hbar w}{\Delta}\right)\left[1+\frac{1}{\varepsilon(\varepsilon+\hbar w/\Delta)}\right] \cdot\left[f(\varepsilon)-f\left(\varepsilon+\frac{\hbar w}{\Delta}\right)\right]d\varepsilon, \tag{18}$$

In a modified normal region

$$\left(\frac{\sigma_{1N'}}{\sigma_{1N}}\right) = \frac{2}{(\hbar w/\Delta)}\int_1^\infty \rho(\varepsilon)\rho\left(\varepsilon+\frac{\hbar w}{\Delta}\right)\left[f(\varepsilon)-f\left(\varepsilon+\frac{\hbar w}{\Delta}\right)\right]d\varepsilon. \tag{19}$$

The plus sign suffix to the conductivity ratio in equation (18) indicates that a plus sign is used in the coherence factor (the first factor enclosed in brackets is the coherence factor); $\hbar w$ is the phonon energy; $f$ is the Fermi function.

Calculating the density-of-state from $\rho(\varepsilon) = (\hbar v_F/\sqrt{3}\,\Delta)\ (dk/d\varepsilon)$ and numerically integrating eq. (18) and (19), either $(\sigma_{1S'}/\sigma_{1N})_+$ or $(\sigma_{1N'}/\sigma_{1N})$ versus $\delta T$ is no longer a smooth, monotonicly decreasing curve as in the case of the BCS calculation.

The line-like energy bands in the region $0 < \varepsilon < 1$ do not make direct

contribution in calculating $(\sigma_{1I}/\sigma_{1N})$, because these lines are found to be much narrower than $\hbar w$ and have the spacing of about $10\,\hbar w$. It is also found that for $\varepsilon > 1$, the influence of the *SNSN*...superlattice becomes important. The computations find sharp bands (band width $< \hbar w$) for $1 < \varepsilon < 1.1$, with band separation $\sim \hbar w$. With increasing $\varepsilon$ the band widths increase, separation remaining of the order of $\hbar w$ up to the value $\varepsilon = 3$. The above mentioned modification in the spectrum is important. From eq. (18) and eq. (19) we realize that in order to have an oscillatory variation of $(\sigma_{1I}/\sigma_{1N})$ within the range $\delta T$ of a few millidegrees, two requirements must be satisfied, namely (1) the density-of-state must vary appreciably within that range of $\delta T$, and (2) $\rho(\varepsilon)$ must vary appreciably in energy of the order $\hbar w$. The new modified spectrum satisfies these two requirements. It is expected that $(\sigma_{1S'}/\sigma_{1N})_+$ and $(\sigma_{1N'}/\sigma_{1N})$ and hence $\alpha_I/\alpha_N$ have on oscillatory structure, and therefore the relation connecting $(\alpha_I/\alpha_N)$ and $(\sigma_{1I}/\sigma_{1N})$ suggests that the dips in $(\sigma_{1S'}/\sigma_{1N})_+$ and $(\sigma_{1N'}/\sigma_{1N})$ versus $\delta T$ will correspond to peaks in the temperature dependence of $\alpha_I/\alpha_N$. In Fig. 2 the calculated dependence of $(\sigma_{1S'}/\sigma_{1N})_+$ and $(\sigma_{1N'}/\sigma_{1N})$ on temperature in the range $0 \leq \delta T \leq 5\,mK$ are shown. Both of them show the same oscillatory structure. The calculation for $(\sigma_{1S'}/\sigma_{1N})_+$ and $(\sigma_{1N'}/\sigma_{1N})$ versus $\delta T$, in Fig. 2 was carried up to $E/\Delta = 3$. Caculation for the higher limit shows the same oscillatory structure. It is seen that the observed attenuation structure coincides rather well with that calculated for $(\sigma_{1S'}/\sigma_{1N})_+$ and $(\sigma_{1N'}/\sigma_{1N})$ from the new theoretical model. The structure in attenuation disappears for values of $\delta T > 5\,mK$, while the calculation of $(\sigma_{1S'}/\sigma_{1N})_+$ and $(\sigma_{1N'}/\sigma_{1N})$ versus $\delta T$ suggests that the structure persists to the value of $\delta T$ greater than $5\,mK$. However, the calculation assumed a demagnetization factor of 1, whereas the disk had a diameter to thickness ratio of less than 10:1. Even on the assumption of an "infinite plate" geometry, for $H = 0.4$ gauss, the $\delta T$ range 0 to $5\,mK$ corresponds to an $H/H_c$ value from 1 to 0.2; and independent studies[10] of the intermediate state have demonstrated that, even for the slanting applied fields, well ordered laminas are not commonly formed for $H/H_c$ values below about 0.2.

**(2) Ultrasonic Attenuation due to Quasiparticles whose Density of States are modified by Single Rectangular Potential Well**

(a) *Density of States of Single Potential Well*

We have attributed the oscillatory structure to the superlattice density

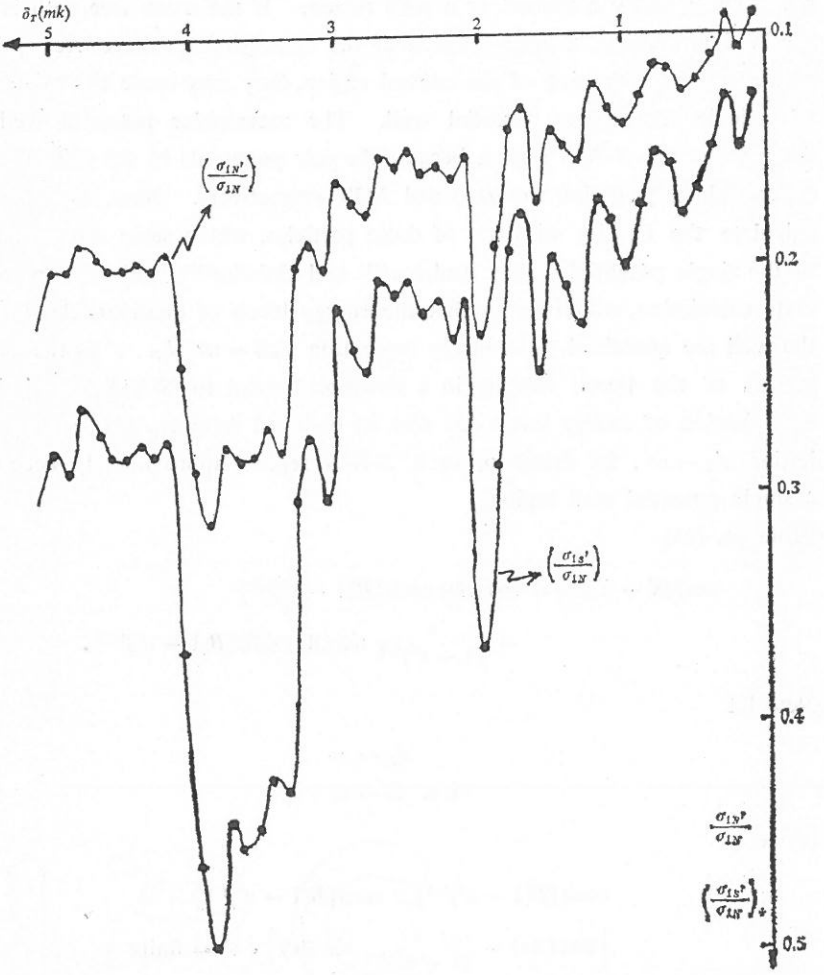


Fig. 2. Conductivity ratio $(\sigma_{IS}'/\sigma_{IN})_+$ and $(\sigma_{IN}'/\sigma_{IN})$ versus $T$ for 105 MHz transverse wave. (The indicated points are numerically integrated, from equations (18) and (19), up to $\epsilon=3$).

of states, as sampled by long free path quasiparticles. Quasiparticles with a short free path will follow the absorption predicted by the geometrical absorption. In geometrical absorption we assume that the density of state in the $N$, $S$ regions are exactly the same as that of pure normal and pure superconducting regions respectively, because of their short free paths they can

only sample either a normal or a pure region. If the mean free path is of the laminar spacing, a large fraction of the quasiparticles have free paths greater than the spacing of the normal region, they may sense the existence of a single rectangular potential well. The rectangular potential well is formed by each *S-N-S* region, because the pair potentials in the normal and superconducting region are zero and $\Delta(T)$ respectively. Now, we have to calculate the density of states of those particles, which sense the existense of the single potential well. Andreev[11] and Galaiko[12] made an approximate calculation, which shows that the energy levels of quasiparticles inside the well are quantized with energy separation $\Delta E = \pi v/d_N$. $v$ is the component of the Fermi velocity in a direction normal to *S-N-S* boundaries. Quantization of energy levels can also be obtained from eq. (14), simply by letting $d_S \to \infty$, by doing so, each *S-N-S* region approximately becomes a single potential well region.

From eq. (14)

$$\cos[(K - k_x)d] = \cos(A\varepsilon)\cosh[B(1-\varepsilon^2)^{1/2}] - \frac{\varepsilon}{(1-\varepsilon^2)^{1/2}}\sin(A\varepsilon)\sinh[B(1-\varepsilon^2)^{1/2}].$$

Now let

$$d_S \to \infty$$
$$\text{i.e. } B \to \infty$$

hence

$$\cosh[B(1-\varepsilon^2)^{1/2}] \simeq \sinh[B(1-\varepsilon^2)^{1/2}] \to \infty$$

$$\therefore \left[\cos(A\varepsilon) - \frac{\varepsilon}{(1-\varepsilon^2)^{1/2}}\sin A\varepsilon\right] \cdot \infty = \text{finite}$$

$$\therefore \cos(A\varepsilon) - \frac{\varepsilon}{(1-\varepsilon^2)^{1/2}}\sin(A\varepsilon) = 0$$

$$\therefore \tan(A\varepsilon) = \frac{(1-\varepsilon^2)^{1/2}}{\varepsilon}. \qquad (20)$$

Thus the values of $\varepsilon$, lying between 0 and $\Delta(T)$, are the roots of the transcendental equation (20), lying between 0 and $\Delta(T)$. These roots, which turn out to be real, and finite in number are the energy levels of those quasiparticles, which sense the existence of a *S-N-S* single potential well. Separation of these energy levels, which are in good agreement with

the value calculated by Andreev and Galaiko, is of order 0.1 $\Delta(T)$. Since the energy separation for $\varepsilon < 1$ is about ten times greater than the ultrasonic phonon energy ($hf$, $f \sim 100$ MHz), they do not contribute directly to the ultrasonic attenuation calculation. Therefore we will concentrate on the contribution obtained from $\varepsilon > 1$ (i. e. $E > \Delta(T)$).

Now, we turn to the Bogolubov equation for a single rectangular potential well (see Fig. 3).

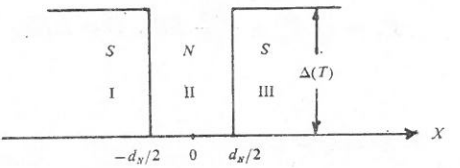


Fig. 3. Single rectangular potential well in the intermediate state.

In region II, $\Delta(T, x) = 0$, the Bogolubov equation becomes

$$\frac{d^2}{dx^2} u(x) + \left(\frac{2mE}{\hbar^2} + k_x\right) u(x) = 0$$
$$\frac{d^2}{dx^2} v(x) + \left(k_x - \frac{2mE}{\hbar^2}\right) v(x) = 0 \qquad (21)$$

The general solution of equation (21) is

$$u_{II}(x) = c_1 \sin(k^+x) + c_2 \cos(k^+x)$$
$$v_{II}(x) = c_3 \sin(k^-x) + c_4 \cos(k^-x) \qquad (22)$$

where

$$k^{\pm} = \left(k_x^2 \pm \frac{2m}{\hbar^2} E\right)^{1/2} \qquad (23)$$

In regions I and III, the Bogolubov equation equation can be written as two coupled differential equations,

$$\frac{d^2}{dx^2} u(x) + \alpha u(x) - \beta v(x) = 0$$
$$\frac{d^2}{dx^2} v(x) + \gamma v(x) - \beta u(x) = 0 \qquad (24)$$

where

$$\alpha = k_x^2 + \frac{2mE}{\hbar^2}, \quad \beta = \frac{2m\Delta}{\hbar^2} \text{ and } \gamma = k_x^2 - \frac{2mE}{\hbar^2}$$

The general solution of equation (24) is

$$u_I(x) = \alpha_1 e^{iP_+x} + \alpha_2 e^{-iP_+x} + \alpha_3 e^{iP_-x} + \alpha_3 e^{-iP_-x}$$

$$v_I(x) = \frac{1}{C}\left[(1-S)(\alpha_1 e^{iP_+x} + \alpha_2 e^{-iP_+x})\right] + \frac{1}{C}\left[(1+S)(\alpha_3 e^{iP_-x} + \alpha_4 e^{-iP_-x})\right] \qquad (25)$$

where

$$P_\pm = \sqrt{k_x^2 \pm \frac{2m}{\hbar^2} ES}\ , \quad C = \Delta/E,$$

and

$$S^2 = 1 - C^2. \qquad (26)$$

Respective general solutions of regions I and III are

$$u_I(x) = C[c_5 e^{iP_+x} + c_6 e^{-iP_+x} + c_7 e^{iP_-x} + c_8 e^{-iP_-x}]$$

$$v_I(x) = (1-S)[c_5 e^{iP_+x} + c_6 e^{-iP_+x}] + (1+S)[c_7 e^{iP_-x} + c_8 e^{-P_-x}] \qquad (27)$$

$$u_{III}(x) = C[c_9 e^{iP_+x} + c_{10} e^{-iP_+x} + c_{11} e^{iP_-x} + c_{12} e^{-iP_-x}]$$

$$v_{III}(x) = (1-S)[c_9 e^{iP_+x} + c_{10} e^{-iP_+x}] + (1+S)[c_{11} e^{iP_-x} + c_{12} e^{-iP_-x}] \qquad (28)$$

The well behaved solutions in regions I, II, III, i. e. equations (22), (27) and (28), are subjected to eight continuity conditons at $x = -d_N/2$ and $x = d_N/2$, namely,

$$u_I(-d_N/2) = u_{II}(-d_N/2)$$
$$v_I(-d_N/2) = v_{II}(-d_N/2)$$
$$u_I'(-d_N/2( = u_{II}'(-d^N/2)$$
$$v_I'(-d_N/2) = v_{II}'(-d_N/2)$$
$$u_{II}(d_N/2) = u_{III}(d_N/2)$$
$$v_{II}(d_N/2) = v_{III}(d_N/2)$$
$$u_{II}'(d_N/2) = u_{III}'(d_N/2)$$
$$v_{II}'(d_N/2) = v_{III}'(d_N/2)$$

where $'$ stands for the first differentiation with respect to $x$. Without going into detailed calculation, we already can see that a solution with 12 undetermined constants subjected to 8 continuity conditions and 3 normalization conditions is an acceptable solution. In other words the spectrum of energy

above $\Delta(T)$ is continuous.

The continuous kinetic energies in region II and III (or I) can be obtained from the corresponding wave vectors, which are given by equations (23) and (26) respectively

$$\frac{\hbar^2 k_{\pm}^2}{2m} = \frac{\hbar^2 k_x^2}{2m} \pm E \tag{29}$$

$$\frac{\hbar^2 P_{\pm}^2}{2m} = \frac{\hbar\, k_x^2}{2m} \pm E\sqrt{1-(\Delta/E)^2} \tag{30}$$

In a pure normal region the kinetic energy is related to the wave vector in a well known form, i. e.

$$E_N = \frac{\hbar^2 k_{\pm}^2}{2m} \left(\text{or } \frac{\hbar^2 P_{\pm}^2}{2m}\right). \tag{31}$$

The density of state in either region II or region III (or I) relative to the pure normal state is given by

$$\rho(E) = \frac{N(E)}{N_N(E)} = \left|\frac{dE_N}{dE}\right|;$$

therefore, from equations (29) and (30) we find

$$\rho_{\text{II}}(E) = \left|\frac{dE_N}{dE}\right| = 1, \tag{32}$$

$$\rho_{\text{I or III}}(E) = \left|\frac{dE_N}{dE}\right| = \sqrt{1-(\Delta/E)^2} + \frac{E}{2\sqrt{1-(\Delta/E)^2}} \cdot \left(\frac{-2\Delta}{E}\right)\left(\frac{-\Delta}{E^2}\right) = \frac{1}{\sqrt{1-(\Delta/E)^2}} = \rho_{BCS}. \tag{33}$$

These results are unexpected, namely the relative density of states in the normal and superconducting region in a rectangular potential well is exactly the same as that of the pure normal and superconducting region for $E > \Delta(T)$.

(b) *Attenuation due to the Energy of a Single Potential Well*

In region (II), $(\sigma_{1N'}/\sigma_{1N})$ can be obtained from equation (19) by substituting $\rho_{\text{II}}(E)$

i. e.,

$$\left(\frac{\sigma_{1N'}}{\sigma_{1N}}\right)_{\text{II}} = \frac{2}{\hbar w}\int_{\Delta}^{\infty} [f(E) - f(E+\hbar w)]\, dE.$$

Because of smallness of the $\hbar w$ i. e. $\hbar w \ll KT$, $(\sigma_{1N'}/\sigma_{1N})_{II}$ becomes

$$\left(\frac{\sigma_{1N'}}{\sigma_{1N}}\right)_{II} \simeq 2\int_{\Delta}^{\infty} -\frac{df}{dE}\,dE = 2f(\Delta) = \frac{2}{\exp(\Delta(T)/KT)+1} \quad (34)$$

Thus, the attenuation in region II is

$$\left(\frac{\alpha_N'}{\alpha_N}\right)_{II} \simeq 1 \Big/ \left(\frac{\sigma_{1N'}}{\sigma_{1N}}\right)_{II} = 1 \Big/ 2f(\Delta)\,. \quad (35)$$

This is a rather interesting result, since $2f(\Delta)$ is less than 1, hence, the attenuation in the normal region of a rectangular potential is predicted to be higher than the pure normal state. Usually the opposite is the case.

We have shown that the density of states of a modified superconducting region (I & III) is exactly the same as that of a pure superconducting state. Therefore, the attenuation can be obtained by using *BCS* density of states in calculation.

From equation (17)

$$\left(\frac{\alpha_{S'}}{\alpha_N}\right)_{I,\,III} = \frac{(\sigma_{1S'}/\sigma_{1N})_{I,\,III}\,(\gamma^2+1)}{(\gamma+\sigma_{2S'}/\sigma_{1N})^2+(\sigma_{1S'}/\sigma_{1N})^2},$$

where

$$\left(\frac{\sigma_{1S'}}{\sigma_{1N}}\right)_{I,\,III} = \left(\frac{\sigma_{1S}}{\sigma_{1N}}\right)_{+} = \frac{2}{\hbar w}\int_{\Delta}^{\infty} \rho_{BCS}(E)\,\rho_{BCS}(E+\hbar w) \cdot\left[1+\frac{\Delta^2}{E(E+\hbar w)}\right][f(E+\hbar w)]dE. \quad (36)$$

The calculation of $(\sigma_{1S}/\sigma_{1N})_{+}$ with approximations appropriate to the case of acoustic waves was made by Cullen and Ferrell[13]

$$\left(\frac{\sigma_{1S}}{\sigma_{1N}}\right)_{+} \simeq 1+\frac{1}{2}\beta\Delta(T)\ln\left(\frac{8\Delta(T)}{e\hbar w}\right)-\left(\frac{7\xi(3)}{\pi^2}\right)(\beta\Delta(T))^2 \quad (37)$$

where $e$ is the base of natural logarithms, $\beta = 1/KT$, $K$ is Boltzmann's constant, $\xi(3)$ is the Riemann zeta function, of numerical value 1.202. From Pippard theory[14]

$$\left(\frac{\sigma_{2S'}}{\sigma_{1N}}\right)_{I,\,III} = \left(\frac{\sigma_{2S}}{\sigma_{1N}}\right) = \frac{hC^2}{\pi e^2 v_S T_C}\,\frac{1}{\lambda^2(0)K_F^2}\,(T_c - T) \quad (38)$$

where

$v_S$: ultrasonic wave velocity

$\lambda(0)$: penetration depth at $T = 0$.

In the present case, $\gamma$ in equation (16) can be written as

$$\gamma = \frac{2\pi c^2 h}{e^2 v_S^3} \left(\frac{f}{K_F}\right)^2 \tag{39}$$

The temperature dependence of $(\alpha_{N'}/\alpha_N)_{II}$ and $(\alpha_{S'}/\alpha_N)_{I,\,III}$ according to the single potential well model are calculated and listed in Table 1.

Table 1. Transverse wave (105M Hz) attenuation ratios versus $\delta_T$, calculated according to a single potential well energy spectrum.

| $\delta_T$(mK) | $(\alpha_{N'}/\alpha_N)_{II}$ | $(\alpha_{S'}/\alpha_N)_{I,III}$ | $\delta_T$(mk) | $(\alpha_{N'}/\alpha_N)_{II}$ | $(\alpha_{S'}/\alpha_N)_{I,III}$ |
|---|---|---|---|---|---|
| 0.1 | 1.047 | 0.8131 | 2.6 | 1.067 | 0.6448 |
| 0.2 | 1.049 | 0.8079 | 2.7 | 1.068 | 0.6373 |
| 0.3 | 1.049 | 1.8026 | 2.8 | 1.068 | 0.6299 |
| 0.4 | 1.050 | 0.7971 | 2.9 | 1.069 | 0.6224 |
| 0.5 | 1.051 | 0.7914 | 3.0 | 1.070 | 0.6151 |
| 0.6 | 1.052 | 0.7856 | 3.1 | 1.070 | 0.6077 |
| 0.7 | 1.053 | 0.7795 | 3.2 | 1.071 | 0.6003 |
| 0.8 | 1.054 | 0.7733 | 3.3 | 1.072 | 0.5930 |
| 0.9 | 1.055 | 0.7665 | 3.4 | 1.072 | 0.5858 |
| 1.0 | 1.055 | 0.7604 | 3.5 | 1.073 | 0.5786 |
| 1.1 | 1.056 | 0.7536 | 3.6 | 1.074 | 0.5714 |
| 1.2 | 1.057 | 0.7470 | 3.7 | 1.074 | 0.5644 |
| 1.3 | 1.058 | 0.7401 | 3.8 | 1.075 | 0.5573 |
| 1.4 | 1.058 | 0.7330 | 3.9 | 1.076 | 0.5503 |
| 1.5 | 1.059 | 0.7260 | 4.0 | 1.076 | 0.5434 |
| 1.6 | 1.060 | 0.7188 | 4.1 | 1.077 | 0.5365 |
| 1.7 | 1.061 | 0.7116 | 4.2 | 1.077 | 0.5297 |
| 1.8 | 1.061 | 0.7043 | 4.3 | 1.078 | 0.5230 |
| 1.9 | 1.062 | 0.6970 | 4.4 | 1.079 | 0.5164 |
| 2.0 | 1.063 | 0.6896 | 4.5 | 1.079 | 0.5098 |
| 2.1 | 1.064 | 0.6822 | 4.6 | 1.080 | 0.5033 |
| 2.2 | 1.064 | 0.6745 | 4.7 | 1.080 | 0.4969 |
| 2.3 | 1.065 | 0.6673 | 4.8 | 1.081 | 0.4905 |
| 2.4 | 1.066 | 0.6598 | 4.9 | 1.082 | 0.4842 |
| 2.5 | 1.066 | 0.6523 | 5.0 | 1.082 | 0.4780 |

(c) *Attenuation due to Deformation Potential Interaction*

Since $\rho(E) = 1$ in a modified normal region, therefore,

$$\left(\frac{\alpha_{N'}}{\alpha_N}\right)_D = \left(\frac{\sigma_{1N'}}{\sigma_{1N}}\right) \simeq \lim_{\hbar w \to 0} \frac{2}{\hbar w} \int_\Delta^\infty [f(E) - f(E + \hbar w)]\, dE$$
$$\simeq 2f(\Delta(T)). \tag{40}$$

We have shown before that the density of states in the modified super state is exactly the same as that of the pure super state, therefore, the attenuation follows the *BCS* derivation:
i. e.

$$\left(\frac{\alpha_{S'}}{\alpha_N}\right)_D = \left(\frac{\sigma_{1S}}{\sigma_{1N}}\right)_- = \frac{2}{\hbar w} \int_\Delta^\infty \frac{E}{(E^2 - \Delta^2)^{1/2}} \frac{(E + \hbar w)}{[(E + \hbar w)^2 - \Delta^2]^{1/2}}$$
$$\cdot \left[1 - \frac{\Delta^2}{E(E + \hbar w)}\right] [f(E) - f(E + \hbar w)]\, dE$$

as before $\hbar w \ll KT$, or $\hbar w \to 0$

$$\left(\frac{\alpha_{S'}}{\alpha_N}\right)_D = \left(\frac{\sigma_{1S}}{\sigma_{1N}}\right)_- \simeq \lim_{\hbar w \to 0} \frac{2}{\hbar w} \int_\Delta^\infty [f(E) - f(E + \hbar w)]\, dE$$
$$\simeq 2f(\Delta(T)). \tag{41}$$

Both attenuations in the modified normal and super states are equal to the attenuation in the pure superconducting state. In other words, according to the single rectangular potential well calculation, attenuation due to deformation potential interaction in the intermediate state is the same as that of the pure superconducting state.

## NUMERICAL CALCULATION

The following equations of the intermediate state have been used in the numerical calculation:

$\rho_N$: fraction of normal region

$$= \frac{d_N}{d} = \frac{h \sin \beta}{(1 - h^2 \cos^2 \beta)^{1/2}}$$

where

$h = H/H_c(T)$

$H = 0.40$ gauss, applied slanting magnetic field, making an acute angle $\beta (= 35°)$ with large surface of the disk specimen.

$H_c(T)$: critical magnetic field at temperature $T$

$$= H_c(0)\left[1 - \frac{T^2}{T_c^2}\right]$$

$T_c$: transition temperature in zero magnetic field.

$$d = d_N + d_S = \left(\frac{e\delta}{\phi(\rho_N)}\right)^{1/2}\left(\rho_N^2 \cot^2\beta + 1\right)^{1/2}$$

: spacing of intermediate laminar

where

$e = 0.1206$ cm, thickness of specimen

$\delta = \delta_0(1 - T/T_c)^{1/2}$, $\delta_0 = 3.3 \times 10^{-5}$ cm for Indium.

$\phi(\rho_N)$: function of normal fraction, has been computed by Lifschitz and Sharvin, and is tabulated in Table 2.

Other numerical values which have been used for Indium are:

$T_c(H = 0) = 3.407$ K

$H_c(0) = 283$ gauss

$K_F = 1.54 \times 10^8$ cm$^{-1}$

$\lambda(0) = 2.38 \times 10^{-6}$ cm

$v_S = 1.035 \times 10^5$ cm/sec.

Numerical values concerning the intermediate state of our Indium sample are listed in Table 3.

Table 2. Function $\phi(\rho_N)$.

| $\rho_N$ | $\rho_S$ | $\phi$ |
|---|---|---|
| 1 | 0 | 0 |
| 0.9 | 0.1 | 0.0020 |
| 0.8 | 0.2 | 0.0065 |
| 0.7 | 0.3 | 0.0128 |
| 0.6 | 0.4 | 0.0182 |
| 0.5 | 0.5 | 0.0221 |
| 0.4 | 0.6 | 0.0224 |
| 0.3 | 0.7 | 0.0195 |
| 0.2 | 0.8 | 0.0136 |
| 0.1 | 0.9 | 0.0055 |
| 0 | 1.0 | 0 |

Table 3. Summarized values in the intermediate state.

| $\delta T$ (mK) | $(d_N/d)$ | $d$ (cm) | $d_N$ (cm) | $d_S$ (cm) | $\Delta(T)$ ($\times 10^{-17}$ erg) |
|---|---|---|---|---|---|
| 0.1 | 0.8942 | 0.4089 | 0.3656 | 0.0433 | 4.282 |
| 0.2 | 0.8166 | 0.2406 | 0.1965 | 0.0441 | 4.359 |
| 0.3 | 0.7542 | 0.1790 | 0.1350 | 0.0440 | 4.435 |
| 0.4 | 0.7026 | 0.1454 | 0.1022 | 0.0433 | 4.509 |
| 0.5 | 0.6591 | 0.1278 | 0.0842 | 0.0436 | 4.582 |
| 0.6 | 0.6216 | 0.1157 | 0.0719 | 0.0438 | 4.654 |
| 0.7 | 0.5889 | 0.1074 | 0.0633 | 0.0442 | 4.725 |
| 0.8 | 0.5601 | 0.1014 | 0.0568 | 0.0446 | 4.794 |
| 0.9 | 0.5344 | 0.0966 | 0.0516 | 0.0450 | 4.863 |
| 1.0 | 0.5113 | 0.0926 | 0.0474 | 0.0453 | 4.931 |
| 1.1 | 0.4904 | 0.0894 | 0.0438 | 0.0456 | 4.998 |
| 1.2 | 0.4714 | 0.0871 | 0.0411 | 0.0461 | 5.064 |
| 1.3 | 0.4541 | 0.0854 | 0.0388 | 0.0465 | 5.129 |
| 1.4 | 0.4381 | 0.0840 | 0.0368 | 0.0472 | 5.194 |
| 1.5 | 0.4233 | 0.0829 | 0.0351 | 0.0478 | 5.257 |
| 1.6 | 0.4096 | 0.0819 | 0.0336 | 0.0484 | 5.320 |
| 1.7 | 0.3969 | 0.0811 | 0.0322 | 0.0489 | 5.382 |
| 1.8 | 0.3850 | 0.0805 | 0.0310 | 0.0495 | 5.443 |
| 1.9 | 0.3739 | 0.0800 | 0.0299 | 0.0501 | 5.504 |
| 2.0 | 0.3635 | 0.0795 | 0.0289 | 0.0506 | 5.564 |
| 2.1 | 0.3537 | 0.0792 | 0.0280 | 0.0512 | 5.624 |
| 2.2 | 0.3444 | 0.0789 | 0.0272 | 0.0518 | 5.682 |
| 2.3 | 0.3357 | 0.0786 | 0.0264 | 0.0522 | 5.740 |
| 2.4 | 0.3274 | 0.0784 | 0.0257 | 0.0527 | 5.798 |
| 2.5 | 0.3196 | 0.0782 | 0.0250 | 0.0532 | 5.855 |
| 2.6 | 0.3121 | 0.0780 | 0.0244 | 0.0537 | 5.912 |
| 2.7 | 0.3050 | 0.0778 | 0.0237 | 0.0541 | 5.967 |
| 2.8 | 0.2983 | 0.0778 | 0.0232 | 0.0546 | 6.023 |
| 2.9 | 0.2919 | 0.0776 | 0.0227 | 0.0550 | 6.078 |
| 3.0 | 0.2857 | 0.0777 | 0.0222 | 0.0555 | 6.132 |
| 3.1 | 0.2798 | 0.0779 | 0.0218 | 0.0561 | 6.186 |
| 3.2 | 0.2742 | 0.0780 | 0.0214 | 0.0566 | 6.240 |
| 3.3 | 0.2688 | 0.0871 | 0.0210 | 0.0571 | 6.293 |
| 3.4 | 0.2637 | 0.0782 | 0.0206 | 0.0576 | 6.345 |
| 3.5 | 0.2687 | 0.0783 | 0.0203 | 0.0580 | 6.397 |
| 3.6 | 0.2539 | 0.0786 | 0.0200 | 0.0587 | 6.449 |
| 3.7 | 0.2493 | 0.0788 | 0.0197 | 0.0592 | 6.500 |
| 3.8 | 0.2449 | 0.0789 | 0.0193 | 0.0595 | 6.551 |
| 3.9 | 0.2407 | 0.0791 | 0.0190 | 0.0600 | 6.602 |
| 4.0 | 0.2365 | 0.0792 | 0.0187 | 0.0604 | 6.652 |
| 4.1 | 0.2326 | 0.0794 | 0.0185 | 0.0609 | 6.702 |
| 4.2 | 0.2288 | 0.0796 | 0.0182 | 0.0614 | 6.751 |
| 4.3 | 0.2251 | 0.0800 | 0.0180 | 0.0620 | 6.800 |
| 4.4 | 0.2215 | 0.0801 | 0.0177 | 0.0623 | 6.849 |
| 4.5 | 0.2180 | 0.0805 | 0.0176 | 0.0629 | 6.897 |
| 4.6 | 0.2147 | 0.0807 | 0.0173 | 0.0633 | 6.945 |
| 4.7 | 0.2114 | 0.0811 | 0.0172 | 0.0640 | 6.993 |
| 4.8 | 0.2083 | 0.0813 | 0.0169 | 0.0644 | 7.040 |
| 4.9 | 0.2052 | 0.0817 | 0.0168 | 0.0649 | 7.087 |
| 5.0 | 0.2023 | 0.0816 | 0.0165 | 0.0651 | 7.134 |

## DISCUSSION

One might ask: "If our model is valid, then why have the present experimental results not already been observed by others[3,4,15]?" There are two considerations here.

(1) Previous intermediate state studies used high magnetic field ($H_c(T)/H_c(0) \sim 0.5$). This means that the intermediate state was studied far away from $T_c(H = 0)$, because the critical field increases with decreasing temperature roughly according to the law

$$H_c(T) = H_c(0)\left[1 - \frac{T^2}{T_c^2(0)}\right].$$

Consequently, the intermediate state in these studies was not examined in the electromagnetic interaction range very close to $T_c$. (This range is only about 10 mK below $T_c(H = 0)$). In our case, our minute field (0.4 G, $H_c(T = 0) = 283$ G) guaranteed that the intermediate state is achieved within the first 10 mK below $T_c(H = 0)$.

(2) According to our new quasiparticle excitation spectrum, the band width and band separation is about $0.01\ \Delta(T)$. Also, because our temperature range is so close to $T_c(0)$, $\Delta(T)$ is sufficiently small that the phonon energy $\hbar w (f \sim 100$ MHz) is of the order of $0.01\ \Delta(T)$. Thus, $\hbar w \sim$ band width $W$ and interband separation $W'$. Now the effect of the band modification is felt strongly, since $\hbar w \sim W, W'$; a significant fraction of the electrons absorbing $\hbar w$ can not find available states and their transitions are forbidden. This implies a reduction of transition probability and a reduction of $(\sigma_{1S'}/\sigma_{1N})_+$ and $(\sigma_{1N'}/\sigma_{1N})$. Therefore, an oscillatory structure of attenuation $\alpha_t$ results.

In previous studies of the intermediate state lower temperatures applied. Hence $\hbar w \ll \Delta(T)$, $\Delta(T)$ changing with $T$ roughly according to the law

$$\Delta(T) = 3.2\ K_B T_c(H = 0)\left[1 - \frac{T}{T_c(H = 0)}\right]$$

Thus $\hbar w \ll$ band width and interband width, and only few electrons contribute to the modified transition probability due to unavailable states in the interband region.

One might also ask whether or not the electrons responsible for the new attenuation mechanism are the electrons in the effective zone. Electrons in the effective zone are those with $\vec{v}_F$ normal to the wave propagation vector $\vec{q}$; hence, if we arrange $\vec{q}$ in the direction parallel to *N–S* intersurfaces, then, the effective zone electrons lie in *NSNS*... planes. Each *NSNS*... plane consists of a *NSNS*... region, therefore, electrons in the effective zone suffer a drastic change in density of states. In other words, electrons in the effective zone are precisely the electrons which are able to contribute to the attenuation of the present model.

## CONCLUSION

(1) The oscillatory structure of transverse ultrasonic attenuation is qualitatively explained.

(2) The transverse wave attenuation of the normal region, due to modification of density of states by *S–N–S* potential well, is higher than that of the pure normal state, and is frequency independent (i. e., $1/(2f(\Delta(T)))$).

(3) Our model also predicts the existence of an oscillatory structure for longitudinal wave attenuation for the intermediate state very near $T_c$, where only the deformation potential interaction is important. In this case, oscillatory variations of attenuation are proportional to $(\sigma_{LN'}/\sigma_{LN})$ and $(\sigma_{LS'}/\sigma_{LN})_-$ for the modified normal and super-state region respectively. Similar to the transverse case, particles responsible for the oscillatory structure are those which sense the *N–S–N–S*... "super-lattice". The experimental verification will be harder than for the transverse wave case, because longitudinal attenuation is much smaller than in the transverse wave case. Furthermore, the longitudinal wave attenuation due to the modification of density of states of particles by the *S–N–S* potential well is exactly the same as that of the pure super conducting state (i. e. $2f(\Delta(T))$).

(4) According to our model, the total attenuation in the intermediate state very near $T_c$, $\alpha_I$, is given by

$$\alpha_I = \alpha_g + \alpha_{sp} + \alpha_{s\ell}$$

where $\alpha_g$ stands for the geometrical attenuation due to particles sensing *N*, *S* regions of the intermediate state as pure normal and pure super conducting states; $\alpha_{sp}$ and $\alpha_{s\ell}$ represent respectively the attenuations due to

particles sensing the *SNS* single potential well and particles sensing the *NSNS*... "super potential lattice". Calculations of $\alpha_g$, $\alpha_{sp}$ and $\alpha_{st}$ are given in our model, therefore, not only the oscillatory structure, but the whole attenuation curve can be verified experimentally in future. A fruitful experimental check of our model is to use samples with various mean free paths. The attenuation of these samples will be different according to our model, because the weight factors of $\alpha_g$, $\alpha_{sp}$ and $\alpha_{st}$ will be different if the mean free path of quasiparticles is changed.

(5) Since both $d_N$ and $d_S$ are not microscopic values, it is possible, but experimentally difficult, to detect either the $d_N$ region or the $d_S$ region separately. Following this suggestion, we can verify the predicted attenuation in either the $N$ region or $S$ region directly.

## ACKNOWLEDGEMENT

This experiment was done at the Catholic University of America during my leave from Fu-Jen University. I would like to thank Professor Jack R. Leibowitz for his enthusiastic help. The experimental research was supported in part by NSF.

Most of numerical calculations were done at the Computer Center, College of Natural Sciences, Fu-Jen University. The use of the facilities of the computer center is highly appreciated. I would also like to thank Mr. Huang Ying-Sheng for part of the numerical calculations.

## REFERENCES

(1) Bardeen J., L. N. Cooper, and J. R. Schrieffer, *Phys. Rev.* **108**, 1175 (1957).
(2) Andreev A. F. and Yu, M. Burk, *JETP* **23**, 942 (1966).
(3) Gottlieb M., C. K. Jones and M. Cerbury, *Phys. Rev. Letters 24A*, 585 (1967).
(4) Singh O. and M. H. Jericho, *Phys. Rev.* **5**, 3542 (1972).
(5) Gottieb M., C. K. Jones and M. Garbuny 1970 *Physical Acoustics* vol. VII ed. W. P. Mason (New York: Academic Press) pp. 1-49.
(6) Leibowitz J. R. and K. Fossheim, *Phys. Rev. Lett.* **21**, 1246 (1968).
(7) Van Gelder A. P., *Phys. Rev.* **181**, 787 (1969).
(8) Fossheim K. and B. Torvain, *J. Low Temperature Phys.* **1**, 341 (1969).
(9) Mattis D. C. and J. Bardeen, *Phys. Rev.* **111**, 412 (1958).
(10) Faber T. E., *Proc. Roy. Soc. (London) A248*, 460 (1958).
(11) Andreev A. F., *JETP* **22**, 455 (1966).
(12) Colaiko V. P., *JETP* **30**, 514 (1970).
(13) Cullen J. R. and R. A. Ferrel, *Phys. Rev.* **146**, 282 (1966).
(14) Pippard A. B., in *Low Temperature Physics*, edited by C. de Witt, B. Breyfus and P. G. de Gennes (Gorden and Breach Publishers, Inc., New York, 1962).
(15) Lea M. J. and E. Read, *J. Phys. F. Metal. Phys.*, Vol. 3, Nov. 3, 1973.

"The right to search for truth implies also a duty; one must not conceal any part of what one has recognized to be true."

EINSTEIN'S CREDO

# STATISTICAL MECHANICS OF NONUNIFORM STELLAR SYSTEMS

KUNG-TUNG WU


## ABSTRACT

The statistical-mechanical description of the nonuniform system is presented. The B-B-G-K-Y hierarchy of equations for the reduced distribution functions are used to derive the kinetic equation for nonuniform stellar systems, but restricted in a finite domain $L_J$, Jeans length. The close collision effects are ignored by a cut-off $L_{\min}$. The mean field is taken as uniform by following a proximate encounter approximation. The Fourier-Laplace transforms and simple contour integrations are performed in calculating the collision operator.


## I. INTRODUCTION

In the history of dynamical studies of star clusters, a number of basic points have become clear. First, Chandrasekhar's[1] theory of stellar encounters has shown that the mean free path in a star cluster is many times the radius of the cluster. Spatial mixing is therefore much more effective than relaxation through stellar encounters, and one may expect the structure of a star cluster to be closely represented by a solution of the encounterless Liouville equation, with stellar encounters producing a slow evolution from one such solution to another. The general solution of the steady-state encounterless Liouville equation was given long ago by Jeans[2].

Since the time of relaxation at the center of a globular cluster is a small fraction of its age, it is natural to look to stellar encounters to provide the regularizing mechanism in star clusters. The dynamics of the encounters which were described by use of the Fokker-Planck equation was provided by Chandrasekhar[3] to calculate the effect of encounters on a velocity distribution of stars. Spitzer and Harm[4] attempted to use the steady-state velocity distribution to derive a cluster model, and Michie[5] derived a distribution function for a spherical stellar system from the Boltzmann equation with encounters. Larson[6] used a numerical analysis to study the secular evolution of star clusters, and the numerical methods which are based upon the Fokker-

Planck equation of Chandrasekhar were developed by Aarseth *et al.*[7]

It has been shown both theoretically (Von Hoerner)[8] and observationally (King)[9] that a star cluster is not unlimited in extent; a finite boundary is set by the tidal force of the Milky Way. Based on steady-state solutions of the Fokker-Planck equation, King[10] presented a dynamical model of star clusters which are spatially limited, corresponding to the tidal cut-off imposed by the Milky Way. The choices of the cut-off are quite insensitive to the divergence of the scattering cross-section of binary encounters in an infinite homogeneous medium, because the divergence is logarithmic. According to Cohen *et al.*[11] it was realized that the Jeans length $L_J$, corresponding to the minimum size of gas clouds which will collapse, provided a more appropriate choice of the cut-off. The finite duration of the encounters was considered by Prigogine and Severne[12], and Ostriker and Davidsen[13]. Other kinetic problems for gravitational systems are treated by Haggerty and Severne[14] and Lerche[15].

A microscopic approach to the kinetic theory of a nonuniform system was taken by Chappell[16] and Prigogine and Severne[17]. The force autocorrelation for the case of a bounded system was discussed by Cohen and Ahmad[18]. The description of encounters in an inhomogeneous system is quite different from the homogeneous case, and the resulting kinetic equations are very difficult to interpret. Thus, in this paper, we attempt to study the kinetic behavior of the nonuniform stellar system, but limited to a finite region. For a finite system, the maximum linear dimension $L$ of the system provides an upper bound to the separation between any two particles and thus appears as a natural cut-off in all collision integrals. This will remove the difficulty of the long range of the gravitational interaction, and leave the self-gravitational field to play the dominant role.

## II. THE B-B-G-K-Y HIERARCHY OF EQUATIONS

Consider our system (cluster) of $N$ particles (stars) with known interaction in a volume V. To concentrate our attention on the volume effects and to minimize the boundary effects, we shall assume the system to be infinite by allowing both $N$ and $V$ to become infinite in such a way that the density $n = N/V$ remains constant. The state of the whole system is described by the probability distribution function in the $6N$-dimensional

space $D_N(X_1, X_2, \cdots, X_N; t)$, where $X_i \equiv (q_i, p_i)$ denotes the coordinates and momenta of the $i$th particle. We take this distribution to be normalized to unity:

$$\int \cdots \int dX_1 \cdots dX_N \, D_N(X_1, \cdots, X_N; t) = 1 . \tag{1}$$

The change of $D_N$ with time is governed by the Liouville equation:

$$\frac{\partial D_N}{\partial t} = [H_N, D_N]_P \equiv \sum_{i=1}^{N} \left( \frac{\partial H_N}{\partial q_i} \cdot \frac{\partial D_N}{\partial P_i} - \frac{\partial H_N}{\partial P_i} \cdot \frac{\partial D_N}{\partial q_i} \right) , \tag{2}$$

where $[\ ,\ ]_P$ is the Poisson bracket, and $H$ is the Hamiltonian of the system,

$$H_N = \sum_{i}^{N} \left[ \frac{1}{2m} P_i^2 + V(q_i) \right] + \sum_{i<j}^{N} \phi( | \vec{q}_i - \vec{q}_j | ) . \tag{3}$$

$V(q_i)$ is the external field on particle $i$, and $\phi( | \vec{q}_i - \vec{q}_j | )$ is the interaction potential. We shall write for brevity

$$\phi_{ij} \equiv \phi( | \vec{q}_i - \vec{q}_j | ) .$$

Now let us define the series of $N$ functions $F_1, F_2, \cdots, F_N$ by

$$F_S(X_1, \cdots, X_S, t) = V^S \int^{N-S} \cdots \int D(X_1, \cdots, X_N; t) \, dX_{S+1} \cdots dX_N . \tag{4}$$

When we integrate Eq. (2) over $X_{S+1}, \cdots, X_N$ and pass to the limit $N \to \infty$, $V \to \infty$, $n = N/V =$ finite, we obtain the so-called B-B-G-K-Y hierarchy of $N$ equations (which were found independently by Bogoliubov, Born and Green, and Kirkwood and Yvon).

$$\frac{\partial F_S}{\partial t} = [H_S, F_S]_P + \frac{N-S}{V} \int dX_{S+1} \left[ \sum_{i=1}^{S} \phi_{i,S+1} , F_{S+1} \right]_P , \tag{5}$$

$$S = 1, 2, \cdots, N$$

where

$$H_S = \sum_{i=1}^{S} \left[ \frac{P_i^2}{2m} + V(q_i) \right] + \sum_{1 \le i < j}^{S} \phi_{ij} .$$

The use of successively simpler distribution functions is made possible by the existence of the widely different characteristic time scale in a system. Here, we consider that the cluster is contained in a stable isolated sphere of radius given in order of magnitude by the Jeans length $L_J$. In a

statistically steady state, we know that $2T + \Omega = 0$[1]. $T$ represents the total kinetic energy of the residual motions (i. e., the motions relative to the center of the cluster), and $\Omega$ is the total mean correlation energy. It is easily shown that the velocity dispersion is

$$\overline{v^2} = \frac{GM}{L_J} = G\rho_0 L_J^2 ,$$

so that

$$L_J = \sqrt{\overline{v^2}}\,(G\rho_0)^{-1/2} ,$$

$G$ being the gravitational constant and $\rho_0$ the mean mass density. Let $\langle m \rangle$ be an average mass of stars, then $L_J^3 \rho_0 \sim N_J \langle m \rangle$. The Jeans number $N_J$ is given by

$$N_J = \frac{L_J^3 \rho_0}{\langle m \rangle} = 0\,(G^{-3/2}) ,$$

$N_J$ can be identified in order of magnitude with the total cluster population: $N_J \sim N$.

The basic characteristic time scales of our system can be distinguished as following:

$t_c$: the duration of a collision: this is the time which a star moving with the average velocity spends in the sphere of influence of another star, $\overline{v}$ being the average velocity of stars, $t_c \simeq L_J/\overline{v}$.

$t_r$: the kinetic relaxation time: this is the time which the system needs to reach some sort of local equilibrium.

$t_h$: the hydrodynamic time: defined as the time necessary for a particle to travel through the hydrodynamic length scale $L_h$.

Let the cluster, at an instant $t = 0$, be in an arbitrary initial state. In a time of order $t_c$, the cluster rapidly changes its state on account of the interstellar interaction $\phi_{ij}$, and the individual star may cross the system many times. This is the violent relaxation stage as described by Lynden-Bell[19]. After a few crossings, the stellar encounters have brought the system to some sort of local equilibrium characterized by a local Maxwellian velocity distribution. This is the so-called kinetic stage. In the further evolution $t > t_r$, when the encounters have brought about some degree of local equilibrium, one can describe the system by the hydrodynamical equa-

tions. This slow secular stage and its secular time scale $t_h$, which is about 2 or 3 orders of magnitude larger than $t_r$, has been studied by Larson[6].

Here, in our system, the ratio of the mean correlation and kinetic energy is

$$\frac{\Omega}{T} \sim \frac{G\langle m\rangle}{L_J \overline{v^2}} = G\langle m\rangle^{2/3} \rho_0^{1/3} \overline{v^2} = N_J^{-2/3} . \tag{6}$$

Obviously, this shows the weakly coupled nature of the system, and thus the characteristic time scale of our system is restricted by the following order: $t_c \ll t_r \ll t_h$.

In the form of the B-B-G-K-Y hierarchy, an approach initiated by Rostoker and Rosenbluth[20] is to have a cluster expansion of $F_2$, $F_3$, ⋯, together with some assumptions on the relative magnitudes of the correction functions and the uncorrelated distribution functions. With these assumptions, we can solve the hierarchy in finite, low orders. The integration of the equations is effected by means of a Fourier-Laplace transform in time.

## III. THE KINETIC EQUATION

Let $F(q_1, p_1; t)\, dq_1\, dp_1 = F(1)\, dX_1$ be the number of stars having coordinates lying between $q_1$ and $q_1 + dq_1$ and momenta between $p_1$ and $p_1 + dp_1$. We expand the many-particle distribution function $F_2$, $F_3$, ⋯, in cluster expansions familiar in equilibrium statistical mechanics, that is

$$F_2(1, 2) = F_1(1)\, F_1(2) + G(1, 2) , \tag{7}$$

$$\begin{aligned} F_3(1, 2, 3) = {} & F_1(1)\, F_1(2)\, F_1(3) + F_1(1)\, G(2, 3) + F_1(2)\, G(3, 1) \\ & + F_1(3)\, G(1, 2) + g(1, 2, 3) . \end{aligned} \tag{8}$$

The term $G(1, 2)$ is the two-particle correlation function, and $g(1, 2, 3)$ is the three-particle correlation. In the following, we shall drop the subscript 1 from $F_1$. The equations for $F$ and $G$ can readily be shown from the B-B-G-K-Y equation (5) to be

$$\begin{aligned} & \left( \frac{\partial}{\partial t} + \vec{v}_1 \cdot \vec{\nabla}_1 + n\vec{K}_1 \cdot \frac{\partial}{\partial \vec{v}_1} \right) F(1) \\ & \quad = n \int \left[ \frac{1}{M_1} \vec{\nabla}_1 \varphi_{12} \cdot \frac{\partial}{\partial \vec{v}_1} - \frac{1}{M_2} \vec{\nabla}_1'' \varphi_{12} \cdot \frac{\partial}{\partial \vec{v}_2} \right] G(1, 2)\, dp_2\, dq_2 , \end{aligned} \tag{9}$$

$$\begin{aligned}
&\left[\frac{\partial}{\partial t}+\vec{v}_1\cdot\vec{\nabla}_1+\vec{v}_2\cdot\vec{\nabla}_2+n\left(\vec{K}_1\cdot\frac{\partial}{\partial\vec{v}_1}+\vec{K}_2\cdot\frac{\partial}{\partial\vec{v}_2}\right)\right]G(1,\,2)\\
&\quad=\vec{\nabla}_1\varphi_{12}\cdot\left(\frac{1}{M_1}\frac{\partial}{\partial\vec{v}_1}-\frac{1}{M_2}\frac{\partial}{\partial\vec{v}_2}\right)[F(1)\,F(2)+G(1,\,2)]\\
&\quad+n\sum_{1=i\neq j}^{2}\frac{1}{M_i}\frac{\partial}{\partial\vec{v}_i}F(i)\cdot\vec{\nabla}_i\int\varphi_{i3}\,G(j,\,3)\,dq_3\,dp_3\\
&\quad+n\sum_{i=1}^{2}\int\frac{1}{M_i}\vec{\nabla}_i\varphi_{i3}\cdot\frac{\partial}{\partial\vec{v}_i}\,g(1,\,2,\,3)\,dq_3\,dp_3\,,
\end{aligned}\tag{10}$$

where $\varphi_{ij}$ is the gravitational potential energy and $\vec{\nabla}_i=\partial/\partial\vec{q}_i$.

For an isolated stable cluster, $\vec{K}_i$ is the self-consistent acceleration field

$$\vec{K}_i\equiv\vec{K}_i(\vec{q}_i,\,t)=-\frac{1}{M_i}\vec{\nabla}_i\int\varphi_{ij}\,F(j)\,dq_j\,dp_j\,.\tag{11}$$

Let us express all lengths in Eqs. (9) and (10) in units of the Jeans length $L_J$. Time will be expressed in unit of $t_c=L_J/\bar{v}$. Further, write the gravitational interaction in the form

$$\varphi_{ij}=-\frac{G\,M_i\,M_j}{|\,\vec{q}_i-\vec{q}_j\,|}=\frac{G\,M_i\,M_j}{L_J}\left(-\frac{L_J}{|\,\vec{q}_i-\vec{q}_j\,|}\right)=\frac{G\,M_i\,M_j}{L_J}\,U_{ij}\,,\tag{12}$$

where $U_{ij}$ is a dimensionless function of the dimensionless distance $|\,\vec{q}_i-\vec{q}_j\,|$. Also, let all $F_S$ be dimensionless functions defined by

$$\begin{aligned}
&\int F_N(dp\,dq)^N=\left(\frac{V}{L_J^3}\right)^N,\\
&F_S=\left(\frac{L_J^3}{V}\right)^{N-S}\int F_N(dp\,dq)^{N-S}\,.
\end{aligned}\tag{13}$$

Then $F$ and $G$ are normalized as above, so that they are dimensionless. Eqs. (9) and (10) then become

$$\begin{aligned}
&\frac{\partial F}{\partial t}+\vec{v}_1\cdot\vec{\nabla}_1F-u_1\frac{\partial F}{\partial\vec{v}_1}\cdot\int\vec{\nabla}_1U_{12}\,F(2)\,dX_2\\
&\quad=\int\left(u_1\nabla_1U_{12}\cdot\frac{\partial}{\partial\vec{v}_1}-u_2\nabla_1U_{12}\cdot\frac{\partial}{\partial\vec{v}_2}\right)G\,dX_2\,,\\
&u_1=\frac{\langle m\rangle}{M_1}\,,\qquad u_2=\frac{\langle m\rangle}{M_2}\,,
\end{aligned}\tag{14}$$

$$\frac{\partial G}{\partial t} + \left[\vec{v}_1 \cdot \vec{\nabla}_2 + \vec{v}_2 \cdot \vec{\nabla}_2 - \epsilon\, \vec{\nabla}_1 U_{12} \cdot \left(u_1 \frac{\partial}{\partial \vec{v}_1} - u_2 \frac{\partial}{\partial \vec{v}_2}\right)\right] G$$
$$= \epsilon\, \vec{\nabla}_1 U_{12} \cdot \left(u_1 \frac{\partial}{\partial \vec{v}_1} - u_2 \frac{\partial}{\partial \vec{v}_2}\right) F(1)\, F(2)$$
$$+ \int dX_3\, F(3) \left(u_1 \vec{\nabla}_1 U_{13} \cdot \frac{\partial}{\partial \vec{v}_1} + u_2 \vec{\nabla}_2 U_{23} \cdot \frac{\partial}{\partial \vec{v}_2}\right) G(1, 2)$$
$$+ \int dX_3 \left[u_1\, G(2, 3)\, \vec{\nabla}_1 U_{13} \cdot \frac{\partial}{\partial \vec{v}_1} F(1) \right. \tag{15}$$
$$\left. + u_2\, G(1, 3)\, \vec{\nabla}_2 U_{23} \cdot \frac{\partial}{\partial \vec{v}_2} F(2)\right]$$
$$+ \int dX_3 \left[u_1 \vec{\nabla}_1 U_{13} \cdot \frac{\partial}{\partial \vec{v}_2} + u_2 \vec{\nabla}_2 U_{23} \cdot \frac{\partial}{\partial \vec{v}_2}\right] g(1, 2, 3)\,,$$

where $\epsilon$ is the dimensionless parameter,

$$\epsilon = \frac{1}{nL_J^3} \sim \frac{1}{N_J} \sim \frac{1}{N} \sim 0(G^{3/2})\,.$$

$\epsilon$ is the reciprocal of the number of stars in a cube of sides equal to the Jeans length $L_J$. The assumption is now made that $G(1, 2)$ is of order $\epsilon$ relative to $F(1)\, F(2)$, and $g(1, 2, 3)$ is of order $\epsilon^2$ relative to $F(1)\, F(2)\, F(3)$, that is

$$\frac{G(1, 2)}{F(1)\, F(2)} = 0(\epsilon) \sim 0(N_J^{-1})\,, \qquad \frac{g(1, 2, 3)}{F(1)\, F(2)\, F(3)} = 0(\epsilon^2) \sim 0(N_J^{-2})\,. \tag{16}$$

We shall note that the assumption Eq. (16) is valid only for the stellar separations that are not too small. For small separations, $\varphi_{ij}$ can become arbitrary large; within the usual approximation where the formation of binaries is neglected, the short separation divergence can be treated by introducing a cut-off.

Neglecting the terms in $g(1, 2, 3)$ and the terms

$$\vec{\nabla}_1 \varphi_{12} \cdot \left(\frac{1}{M_1} \frac{\partial}{\partial \vec{v}_1} - \frac{1}{M_2} \frac{\partial}{\partial \vec{v}_2}\right) G(1, 2)$$

in Eq. (10) since they appear in higher order in $\epsilon$ in Eq. (15), we find that Eqs. (9) and (10) become a closed pair of equations for $F$ and $G$.

$$\left(\frac{\partial}{\partial t} + \vec{v}_1 \cdot \vec{\nabla}_1 + n\vec{K}_1 \cdot \frac{\partial}{\partial \vec{v}_1}\right) F(1)$$
$$= n \int \left(\frac{1}{M_1} \vec{\nabla}_1 \varphi_{12} \cdot \frac{\partial}{\partial \vec{v}_1} - \frac{1}{M_2} \vec{\nabla}_1 \varphi_{12} \cdot \frac{\partial}{\partial \vec{v}_2}\right) G(1, 2)\, dp_2\, dq_2\,, \tag{17}$$

$$\left[\frac{\partial}{\partial t}+\vec{v}_1\cdot\vec{\nabla}_1+\vec{v}_2\cdot\vec{\nabla}_2+n\left(\vec{K}_1\cdot\frac{\partial}{\partial\vec{v}_1}+\vec{K}_2\cdot\frac{\partial}{\partial\vec{v}_2}\right)\right]G(1,2)$$
$$=\vec{\nabla}_1\varphi_{12}\cdot\left(\frac{1}{M_1}\frac{\partial}{\partial\vec{v}_1}-\frac{1}{M_2}\frac{\partial}{\partial\vec{v}_2}\right)F(1)F(2) \tag{18}$$
$$+n\sum_{1=i\neq j}^{2}\frac{1}{M_i}\frac{\partial}{\partial\vec{v}_i}F(i)\cdot\vec{\nabla}_i\int\varphi_{i3}G(j,3)\,dp_3\,dq_3\,.$$

The left-hand side of Eq. (17) gives the stream and the Vlasov terms, and the right-hand side yields the correlation or collective effects. The terms containing $\vec{K}_1$ and $\vec{K}_2$ on the left-hand side of Eq. (18) come from the three-particle effects.

The procedures which are developed above are familiar from plasma theory. As we know in plasma theory, it is a good approximation to consider the system as spatially homogeneous, because of the short range interaction due to the Debye-Hückel screening which is responsible for the long-range divergence. In this case, the $\vec{v}_1\cdot\vec{\nabla}_1$ term and the Vlasov term in Eq. (17) vanish. The two terms containing $\vec{K}_1$ and $\vec{K}_2$ in Eq. (18) also vanish. Then Eq. (18) can be solved explicity.

But in the gravitational system, unlike the plasma, there is no tendency toward homogeneity, so that the inhomogeneity cannot be ignored, and the self-gravitational field always plays a dominant role. This leads us to use an alternative approximation by omitting the collective effect terms

$$n\sum_{1=i\neq j}^{2}\frac{1}{M_i}\frac{\partial}{\partial\vec{v}_i}F(i)\cdot\vec{\nabla}_i\int\varphi_{i3}G(j,3)\,dq_3\,dp_3$$

in Eq. (18). They will not be important in a stable system, just as the vibration modes, being too strongly damped, are not significant in the collisional processes of a non-rotating system[21]. The field terms $\vec{K}(\vec{q}_i,t)$ which appear in Eqs. (17) and (18) can be understood by the following argument. In a few crossing times $t_c=L_J/\bar{v}$, the cluster will undergo the evolution from the violent mixing stage to the slow and smooth secular stage. The self-consistent field $\vec{K}(\vec{q}_i,t)$ will also approach the mean field $\overline{\vec{K}(\vec{q}_i,t)}\equiv\overline{\vec{K}_i}$ which varies only on the secular time scale $t_h$. So, in the intermediate kinetic stage ($t_r\ll t_h$) which is of interest here, the mean field $\overline{\vec{K}_i}$ can be treated as a stationary field of spatial variation $\overline{\vec{K}(\vec{q}_i,t)}=\overline{\vec{K}(\vec{q}_i)}$.

Therefore, Eqs. (17) and (18) become the reduced form

$$\left(\frac{\partial}{\partial t}+\vec{v}_1\cdot\vec{\nabla}_1+n\overline{\vec{K}(\vec{q}_1)}\cdot\frac{\partial}{\partial\vec{v}_1}\right)F(1)$$
$$=n\int\left[\frac{1}{M_1}\vec{\nabla}_1\varphi_{12}\cdot\frac{\partial}{\partial\vec{v}_1}-\frac{1}{M_2}\vec{\nabla}_1\varphi_{12}\cdot\frac{\partial}{\partial\vec{v}_2}\right]G(1,2)\,dp_2\,dq_2\,, \tag{19}$$

$$\left[\frac{\partial}{\partial t}+\vec{v}_1\cdot\vec{\nabla}_1+\vec{v}_2\cdot\vec{\nabla}_2+n\left(\vec{K}(\vec{q}_1)\cdot\frac{\partial}{\partial\vec{v}_1}+\vec{K}(\vec{q}_2)\cdot\frac{\partial}{\partial\vec{v}_2}\right)\right]G(1,2)$$
$$=\vec{\nabla}_1\varphi_{12}\cdot\left(\frac{1}{M_1}\frac{\partial}{\partial\vec{v}_1}-\frac{1}{M_2}\frac{\partial}{\partial\vec{v}_2}\right)F(1)\,F(2)\,. \tag{20}$$

If we use the velocity variable $\vec{v}_i$, instead of the momentum variable $\vec{P}_i$, and the velocity distribution functions $f_1, f_2, \cdots$, instead of the reduced distribution functions $F_1, F_2, \cdots$, in Eqs. (19) and (20), the connections between these functions are given by

$$f_1(\vec{x},\ \vec{v},\ t)\,d^3v=n\,F_1(\vec{q},\ \vec{p},\ t)\,d^3p\,, \tag{21}$$

$$f_2(\vec{x}_1,\ \vec{v}_1,\ \vec{x}_2,\ \vec{v}_2,\ t)\,d^3v_1\,d^3v_2=n^2\,F_2\,(\vec{q}_1,\ \vec{p}_1,\ \vec{q}_2,\ \vec{p}_2,\ t)\,d^3p_1\,d^3p_2\,. \tag{22}$$

Here, we use $\vec{x}_i$, instead of $\vec{q}_i$, to represent the position variable. Define the particle interaction operator $\theta_{ij}$ by

$$\theta_{ij}=\frac{\partial\varphi_{ij}}{\partial\vec{x}_i}\cdot\frac{\partial}{\partial\vec{p}_i}+\frac{\partial\varphi_{ij}}{\partial\vec{x}_j}\cdot\frac{\partial}{\partial\vec{p}_j}$$
$$=(\vec{\nabla}_i\varphi_{ij})\cdot\partial_{ij}\,, \tag{23}$$

where

$$\partial_{ij}=\frac{1}{M_i}\frac{\partial}{\partial\vec{v}_i}-\frac{1}{M_j}\frac{\partial}{\partial\vec{v}_j}\,,$$

and the linear, time-independent operator $\mathcal{L}_i$ in the mean field by

$$\mathcal{L}_i=\vec{v}_i\cdot\vec{\nabla}_i+\overline{\vec{K}(\vec{x}_i)}\cdot\frac{\partial}{\partial\vec{v}_i}\,,\qquad\text{where}\quad\vec{\nabla}_i=\frac{\partial}{\partial\vec{x}_i}\,.$$

Then, from Eqs. (19) and (20) the kinetic equations for the weakly coupled encounter become

$$\left(\frac{\partial}{\partial t}+\mathcal{L}_1\right)f(1)=\int d\vec{v}_2\,d\vec{x}_2\,\theta_{12}\,g(1,2) \tag{24}$$

and

$$\left(\frac{\partial}{\partial t} + \mathcal{L}_1 + \mathcal{L}_2\right) g(1, 2) = \theta_{12} f(1) f(2) . \tag{25}$$

Now

$$f(1) \equiv f(\vec{x}_1, \vec{v}_1, t) , \quad f(2) \equiv f(\vec{x}_2, \vec{v}_2, t) ,$$
$$g(1, 2) \equiv g(\vec{x}_1, \vec{v}_1, \vec{x}_2, \vec{v}_2, t) .$$

## IV. THE NON-MARKOVIAN EVOLUTION EQUATIONS

For the free uncorrelated motion in the mean field, the solution of the Liouville equation can be written formally:

$$f(\vec{x}_i, \vec{v}_i, t) = e^{-\mathcal{L}_i t} f(\vec{x}_i, \vec{v}_i, 0) = e^{-\mathcal{L}_i t} \tilde{f}(\vec{x}_i, \vec{v}_i, t) . \tag{26}$$

The meaning of Eq. (26) is that the value of $f$ at $t$ when the phase of the system is $\vec{x}_i$, $\vec{v}_i$, is the same as that when the phase is $e^{-\mathcal{L}_i t}\vec{x}_i$, $e^{-\mathcal{L}_i t}\vec{v}_i$.

The formal solution of Eq. (25) can be written:

$$\begin{aligned} g(1, 2) &= e^{-t(\mathcal{L}_1+\mathcal{L}_2)} g(1, 2, t = 0) \\ &\quad + e^{-t(\mathcal{L}_1+\mathcal{L}_2)} \int_0^t d\tau\, \theta_{12}\, e^{-\tau(\mathcal{L}_1+\mathcal{L}_2)} \tilde{f}(1, t - \tau) \tilde{f}(2, t - \tau)\, e^{\tau(\mathcal{L}_1+\mathcal{L}_2)} . \end{aligned} \tag{27}$$

Substituting Eq. (27) into Eq. (24), we obtain the evolution equation

$$\begin{aligned} \left(\frac{\partial}{\partial t} + \mathcal{L}_1\right) f(1) &= e^{-\mathcal{L}_1 t} \frac{\partial}{\partial t} \tilde{f}(1, t) \\ &= D(1, t) + e^{-t(\mathcal{L}_1+\mathcal{L}_2)} \int_0^t d\tau \int d\vec{r}_2 d\vec{v}_2\, \Lambda_{12} \tilde{f}_1(1, t - \tau) \tilde{f}_2(2, t - \tau), \end{aligned} \tag{28}$$

where

$$D(1, t) = \int \theta_{12}\, e^{-t(\mathcal{L}_1+\mathcal{L}_2)}\, g(1, 2, t = 0)\, d\vec{x}_2\, d\vec{v}_2 , \tag{29}$$

$$\Lambda_{12} = \theta_{12}\, e^{-\tau(\mathcal{L}_1+\mathcal{L}_2)}\, \theta_{12}\, e^{\tau(\mathcal{L}_1+\mathcal{L}_2)} . \tag{30}$$

Equation (28) shows very clearly how the effect of the initial condition at time $t = 0$ ($D(1, t)$) and the effect of the correlation $\Lambda_{12}$ at all times $\tau < t$ are propagated toward time $t$. It is seen that only the behavior of the correlation at times $\tau$ earlier than $t$ can influence the value of $f(1)$ at time $t$. This is the so-called non-Markovian relation.

In order to take the delocalization effects into account, we can rewrite the collision operator by using the properties of the $\delta$ function, as

$$\Lambda_{12} = \theta_{12} \int e^{-\tau(\mathcal{L}_1' + \mathcal{L}_2')} \frac{\partial \varphi_{12}(r')}{\partial \vec{r}'} \cdot \partial_{12}\, e^{\tau(\mathcal{L}_1 + \mathcal{L}_2)} \times \delta(\vec{x}_1' - \vec{x})\, \delta(\vec{v}_1' - \vec{v})\, \delta(\vec{x}_2' - \vec{x}_2)\, \delta(\vec{v}_2' - \vec{v}_2)\, d\vec{x}_1'\, d\vec{x}_2'\, d\vec{v}_1'\, d\vec{v}_2' , \tag{31}$$

where

$$\vec{r}' = \vec{x}_1' - \vec{x}_2' , \qquad \vec{\nabla}_i' = \frac{\partial}{\partial \vec{r}'} ,$$

and

$$\mathcal{L}_i' = \vec{v}_i' \cdot \vec{\nabla}_i' + \overline{\vec{F}(\vec{x}_i')} \cdot \frac{\partial}{\partial \vec{v}_i'} .$$

The mean field $\overline{\vec{K}(\vec{x}_i)}$ which varies on the scale $L_J$ can be taken as uniform in the limit of stellar separations $r_0 \ll L_J$, $r_0$ being a characteristic distance over which the field variation can be ignored. In the stellar encounter, we may expect that the major contribution to the collision term comes from the proximate pair separation $r$ such that $r < r_0 \ll L_J$. The small contribution which comes from distant stars should affect the mean field as an error. This approximative treatment of the field constitutes a proximate encounter approximation which is suggested by Severne and Haggerty[22]. This approximation concerns only the treatment of the correlations.

With this assumption, it is possible to take the mean field $\overline{\vec{K}(\vec{x}_i)}$ as uniform in the collision operator $\Lambda_{12}$. Thus, it is easily shown that Eq. (31) becomes

$$\Lambda_{12} = \theta_{12} \int e^{-[\tau(v_1' - v_2') \cdot \partial / \partial r']} \frac{\partial \varphi_{12}(r')}{\partial \vec{r}'} \cdot (\partial_{12} + \tau \vec{\nabla}_{12}) , \tag{32}$$

where

$$\vec{\nabla}_{12} = \vec{\nabla}_1 - \vec{\nabla}_2 .$$

Therefore, Eq. (28) can be written as

$$e^{-\mathcal{L}_1 t} \frac{\partial \tilde{f}(1, t)}{\partial t} = D(1, t) + \int d\vec{x}_2\, d\vec{v}_2 \int dr\, \delta[\vec{r} - (\vec{x}_1 - \vec{x}_2)] \cdot \int_0^t \frac{d\tau}{8\pi^3}\, \Lambda(\vec{r}, \tau)\, e^{-(\mathcal{L}_1 + \mathcal{L}_2)t}\, \tilde{f}(1, t - \tau)\, \tilde{f}(2, t - \tau) , \tag{33}$$

with

$$\Lambda(\vec{r},\ \tau) = 8\pi^3\,\theta_{12}(\vec{r})\,(e^{-\tau\vec{v}_{12}\cdot\partial/\partial\vec{r}})\left[\,\theta_{12}(\vec{r}) + \tau\,\frac{\partial\varphi_{12}}{\partial\vec{r}}\cdot\vec{\nabla}_{12}\right],$$
$$\vec{r} = \vec{x}_1 - \vec{x}_2\,, \qquad \theta_{12}(r) = \frac{\partial\varphi_{12}}{\partial\vec{r}}\cdot\partial_{12}\,, \qquad \vec{v}_{12} = \vec{v}_1 - \vec{v}_2\,. \tag{34}$$

In our finite system, we assume that the cluster is contained in a sphere of radius given in order of magnitude by the Jeans length $L_J$. With this natural cut-off, one could write

$$\varphi_{12}(\,|\,\vec{x}_1 - \vec{x}_2\,|\,) = \begin{cases} \gamma\,|\,\vec{x}_1 - \vec{x}_2\,|^{-1} & \text{for } x_1 \le L_J \text{ and } x_2 \le L_J\,, \\ 0 & \text{for } x_1 \text{ or } x_2 > L_J\,, \end{cases} \tag{35}$$

where $\gamma = -GM_1M_2$. This idealized $1/r$ potential with a cut-off at $r = L_J$ can realistically be replaced by the screened potential (just as the Debye potential in plasma)

$$\varphi_{12}(r) = \gamma\,\frac{e^{-kr}}{r}\,, \qquad \text{where } k = \frac{2\pi}{L_J}\,.$$

Equations (33) and (34) are to be integrated by use of the Laplace transform in $t$ and the Fourier transform in $r$. The Fourier integral transform $\varphi_1^{q^2}$ of the potential is

$$\varphi_{12}^{q} = \left(\frac{1}{2\pi}\right)^3\int_{-\infty}^{\infty}\varphi_{12}(r)\,e^{-i\vec{q}\cdot\vec{r}}\,dr = \frac{\gamma}{2\pi^2}\,\frac{1}{q^2 + k^2}\,, \tag{36}$$

$$\varphi_{12}(r) = \int dq\,\varphi_{12}^{q}\,e^{i\vec{q}\cdot\vec{r}} = \int d\vec{q}\,\frac{\gamma}{2\pi^2}\,\frac{e^{i\vec{q}\cdot\vec{r}}}{(q^2 + k^2)}\,, \tag{37}$$

and the Laplace transformation is

$$\Phi(t) = \int\frac{dz}{-2\pi}\,e^{-izt}\,\phi(z)\,, \qquad \phi(z) = \int_0^{\infty}dt\,e^{izt}\,\Phi(t)\,. \tag{38}$$

The contour for the $z$-integration is a line antiparallel to and just above the real axis.

Here, in the non-uniform system, we use $\vec{\ell}$ and $(\vec{\ell} - \vec{q})$ to represent two different wave vectors associated with the interaction energy. Therefore, the Fourier integral transforms become

$$\varphi_{12}^{(1)}(r) = \int d\vec{\ell}\,\varphi_{12}^{\ell}\,e^{i\vec{\ell}\cdot\vec{r}} = \int d\vec{\ell}\,\frac{\gamma}{2\pi^2}\,\frac{e^{i\vec{\ell}\cdot\vec{r}}}{(\ell^2 + k^2)}\,, \tag{39}$$

$$\varphi_{12}^{(2)}(r) = \int d(\vec{\ell} - \vec{q})\,\varphi_{12}^{\ell-q}\,e^{i(\vec{\ell}-\vec{q})\cdot\vec{r}} = \int d(\vec{\ell} - \vec{q})\,\frac{\gamma}{2\pi^2}\,\frac{e^{i(\vec{\ell}-\vec{q})\cdot\vec{r}}}{[(\vec{\ell} - \vec{q})^2 + k^2]}\,. \tag{40}$$

Substituting Eqs. (39) and (40) and applying the Laplace transform into Eq. (34), the collision operator can be written as

$$\begin{aligned}\Lambda(\vec{r},\tau) &= \int \frac{dz}{-2\pi z}\, e^{-iz\tau} \int_0^\infty d\tau\, e^{iz\tau}\, \Lambda(\vec{r},\,\tau) \\ &= \int \frac{dz}{-2\pi z}\, e^{-iz\tau} \int_0^\infty d\tau\, e^{iz\tau}\, 8\pi^3 \frac{\partial \varphi_{12}^{(2)}(r)}{\partial \vec{r}} \\ &\quad \cdot \partial_{12}\, e^{-\tau \vec{v}_{12}\cdot \partial/\partial \vec{r}} \left[ \frac{\partial \varphi_{12}^{(1)}(r)}{\partial \vec{r}} \cdot \partial_{12} + \tau \left( \frac{\partial \varphi_{12}^{(1)}(r)}{\partial \vec{r}} \right) \cdot \vec{\nabla}_{12} \right].\end{aligned} \tag{41}$$

Using

$$\frac{\partial \varphi_{12}^{(2)}}{\partial \vec{r}} = \int d(\vec{\ell} - \vec{q})\, i(\vec{\ell} - \vec{q})\, \varphi_{12}^{\ell - q}\, e^{i(\vec{\ell} - \vec{q})\cdot \vec{r}},$$

$$\frac{\partial \varphi_{12}^{(1)}}{\partial \vec{r}} = \int d\vec{\ell}\, i\vec{\ell}\, \varphi_{12}^{\ell}\, e^{i\vec{\ell}\cdot \vec{r}},$$

and

$$\int_0^\infty dz\, e^{-i\tau(\vec{\ell}\cdot \vec{v}_{12} - z)} = \frac{1}{i(\vec{\ell}\cdot \vec{v}_{12} - z)}.$$

Eq. (41) becomes

$$\begin{aligned}\Lambda(\vec{r},\,\tau) &= \int \frac{dz}{-2\pi} e^{-iz\tau}\, 8\pi^3 \int d(\vec{\ell} - \vec{q})\, i(\vec{\ell} - \vec{q})\, \varphi_{12}^{\ell - q}\, e^{i(\vec{\ell} - \vec{q})\cdot \vec{r}} \\ &\quad \cdot \partial_{12} \left[ \frac{\int d\vec{\ell}\, i\vec{\ell}\, \varphi_{12}^{\ell}}{i(\vec{\ell}\cdot \vec{v}_{12} - z)} \cdot \partial_{12} - \frac{\partial}{\partial \vec{v}_{12}} \int d\vec{\ell}\, \varphi_{12}^{\ell} \frac{1}{i(\vec{\ell}\cdot \vec{v}_{12} - z)} \cdot \vec{\nabla}_{12} \right].\end{aligned} \tag{42}$$

Then it is easily shown that

$$\begin{aligned}\Lambda(\vec{r},\,\tau) &= \int \frac{dz}{-2\pi} e^{-iz\tau} \int d\vec{q}\, e^{i\vec{q}\cdot \vec{r}}\, 8\pi^3 \int d\vec{\ell}\, \varphi_{12}^{\ell - q}(\vec{\ell} - \vec{q}) \\ &\quad \cdot \partial_{12} \frac{-i}{(\vec{\ell}\cdot \vec{v}_{12} - z)} \left[ \varphi_{12}^{\ell}\, \vec{\ell}\cdot \partial_{12} - \frac{i}{(\vec{\ell}\cdot \vec{v}_{12} - z)} \varphi_{12}^{\ell}\, \vec{\ell}\cdot \vec{\nabla}_{12} \right] \\ &= \int \frac{dz}{-2\pi} e^{-iz\tau} \int d\vec{q}\, e^{i\vec{q}\cdot \vec{r}}\, \Lambda_{\vec{q}}(z),\end{aligned} \tag{43}$$

where

$$\begin{aligned}\Lambda_{\vec{q}}(z) &= 8\pi^3 \int d\vec{\ell}\, \frac{\gamma(\vec{\ell} - \vec{q})}{2\pi^2[(\vec{\ell} - \vec{q})^2 + k^2]} \cdot \partial_{12} \frac{-i}{(\vec{\ell}\cdot \vec{v}_{12} - z)} \times \\ &\quad \left[ \frac{\gamma}{2\pi^2(\ell^2 + k^2)}\, \vec{\ell}\cdot \partial_{12} - \frac{i}{(\vec{\ell}\cdot \vec{v}_{12} - z)} \frac{\gamma}{2\pi^2(\ell^2 + k^2)}\, \vec{\ell}\cdot \vec{\nabla}_{12} \right] \\ &= \gamma^2 \partial_{12} \left\{ [\vec{I}^{(2)} - \vec{q}\vec{I}^{(1)}] \cdot \partial_{12} - i[\partial(\vec{I}^{(2)} - \vec{q}\vec{I}^{(1)})/\partial z] \cdot \vec{\nabla}_{12} \right\}.\end{aligned} \tag{44}$$

Here, we introduce the integrated form of the tensor quantities

$$\vec{I}^{(n)}(z) = \frac{2}{i\pi} \int d\vec{\ell}\, \frac{1}{(\vec{\ell} \cdot \vec{v}_{12} - z)} \frac{(\vec{\ell})^n}{[(\vec{\ell} - \vec{q})^2 + k^2][\ell^2 + k^2]}, \quad n = 1, 2. \tag{45}$$

Therefore, from Eq. (43), the non-Markovian evolution equation (33) becomes

$$\begin{aligned} e^{-\mathcal{L}_1 t} \frac{\partial \tilde{f}(1, t)}{\partial t} &= D(1, t) + \int d\vec{x}_2\, d\vec{v}_2 \int_0^t \frac{d\tau}{8\pi^3} \int \frac{dz}{-2\pi}\, e^{iz\tau} \\ &\times \int d\vec{q}\, e^{i\vec{q}\cdot(\vec{x}_1 - \vec{x}_2)}\, \Lambda_{\vec{q}}(z)\, e^{-\tau(\mathcal{L}_1 + \mathcal{L}_2)} \tilde{f}(1, t - \tau) \tilde{f}(2, t - \tau). \end{aligned} \tag{46}$$

Then Eqs. (44) and (46) provide a corrective description of the evolution of the system.

## V. THE CALCULATION OF THE INTEGRATED FORM $\vec{I}^{(n)}(z)$ AND THE COLLISION OPERATOR $\Lambda_{\vec{q}}(z)$

Consider now the function $I^{(n)}(z)$, defined by Eq. (45). This function is a typical Cauchy integral. One of its main properties is the fact that it represents two different functions, according to whether the complex variable $z$ lies in the upper or in the lower half-plane; these two functions will be called $\vec{I}^{(n)+}$ and $\vec{I}^{(n)-}$, respectively. Each of them is regular in the domain of its original definition. However, $\vec{I}^{(n)-}$ is not the analytical continuation of $\vec{I}^{(n)+}$, there is a discontinuity along the whole real axis. On the other

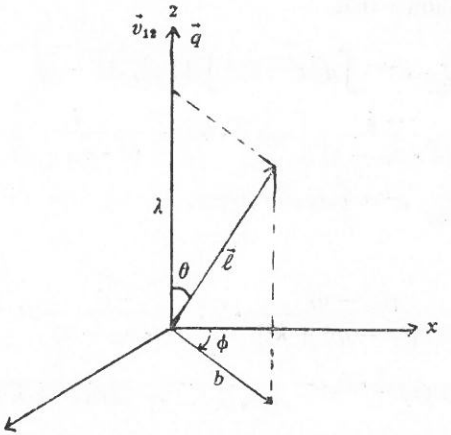


Fig. 1. Cylindrical Polar Coordinates for Wave Vectors $\vec{\ell}$ and $\vec{q}$

hand, the function $\vec{I}^{(n)+}$ can in general be continued analytically into the lower half-plane. The function $\vec{I}^{(n)+}(z)$ thus defined in the whole complex plane necessarily will have singularities in the lower half-plane.

The calculation is particularly convenient in a reference system $(x, y, z)$ in which the $z$-axis is directed along the vector $\vec{v}_{12}$. The calculation may then be performed by using cylindrical coordinates. The cylindrical polar coordinates for $\vec{\ell}$ are $\ell_z = \lambda$, $b$ and $\phi$. For simplicity and practicability, we may assume that $\vec{q}$ is also along the $z$-axis (see Fig. 1).

From parity arguments we know that the tensor $\vec{I}^{(n)+}$ is diagonal in this reference system, and that, moreover, the $xx$ and $yy$ components are equal.

Now, let us evaluate $\vec{I}^{(1)}(z)$, and introduce the notation

$$I^{(1)}(z) = \vec{I}_1^{(1)}(z)\,(\hat{\ell}_x + \hat{\ell}_y) + I_2^{(1)}(z)\,\hat{\ell}_z\,,$$
$$\ell^2 = b^2 + \lambda^2\,, \qquad \ell_y = b\sin\phi\,, \qquad \ell_z = \lambda\,.$$

From Eq. (45), it becomes

$$\vec{I}^{(1)}(z) = \frac{2}{i\pi}\int d\vec{\ell}\,\frac{1}{\vec{\ell}\cdot\vec{v}_{12} - z}\,\frac{\vec{\ell}}{[\ell^2 + k^2][(\vec{\ell} - \vec{q})^2 + k^2]}\,. \tag{47}$$

The integral over $\vec{\ell}$ in Eq. (47) is logarithmically divergent at the upper limit. This divergence for $\vec{\ell} \to \infty$ is a short-distance divergence. Such behavior can be shown to be general for the potential which becomes infinite at very short distances ($\varphi(r) \to \infty$ as $r \to 0$). We shall treat this difficulty much more roughly, by cutting off the domain of integration at a value $\ell_{\max} = \ell_M$. Now, we discuss a reasonable value for the choice of the cut-off $\ell_M$, although there is a certain arbitrariness in this choice. As the physical reason for the divergence at the upper limit is the strong interaction at short distances, we have to eliminate very close encounters, which produce large deflections. We may set a limit of weak deflection at 90°. It can be shown from a simple analysis of the dynamics of a collision[23] that such a deflection occurs when the potential energy at a distance equal to the impact parameter $L_{\min}$ equals twice the original kinetic energy:

$$2\left(\frac{M_1 M_2}{M_1 + M_2}\right)\frac{v_{12}^2}{2} = \frac{e^{-kL_{\min}}}{L_{\min}}\,(-GM_1M_2)\,. \tag{48}$$

Since presumably $L_{\min}^{-1} \gg k$, the exponential factor approximately equals 1. From Eq. (48) we obtain $L_{\min} = G(M_1 + M_2)/v_{12}^2$. We then choose for $\ell_M$

$$\ell_M = \frac{2\pi}{L_{\min}} = \frac{2\pi v_{12}^2}{G(M_1 + M_2)} \approx N_J k . \tag{49}$$

With this cut off at $\ell = \ell_M$, we can write $I_1^{(1)}(z)$ and $I_2^{(1)}(z)$ from Eq. (47) as

$$\begin{aligned} I_1^{(1)}(z) = \frac{2}{i\pi} \int_{-\infty}^{\infty} d\lambda \, \frac{1}{\lambda v_{12} - z} \int_0^{\ell_M} bdb \\ \times \int_0^{2\pi} d\phi \, \frac{b \sin\phi}{[b^2 + \lambda^2 + k^2][b^2 + (\lambda - q)^2 + k^2]} = 0 , \end{aligned} \tag{50}$$

$$\begin{aligned} I_2^{(1)}(z) &= \frac{2}{i\pi} \int_{-\infty}^{\infty} d\lambda \, \frac{1}{\lambda v_{12} - z} \int_0^{\ell_M} bdb \\ &\quad \times \int_0^{2\pi} d\phi \, \frac{\lambda}{[b^2 + \lambda^2 + k^2][b^2 + (\lambda - q)^2 + k^2]} \\ &= \frac{2}{i} \int_{-\infty}^{\infty} d\lambda \, \frac{1}{\lambda v_{12} - z} \, \frac{1}{q(q - 2\lambda)} \\ &\quad \times \left[ \log \frac{\ell_M^2 + \lambda^2 + k^2}{\ell_M^2 + k^2 + (\lambda - q)^2} - \log \frac{\lambda^2 + k^2}{[(\lambda - q)^2 + k^2]} \right] . \end{aligned} \tag{51}$$

From Eq. (49), $k/\ell_M \sim N_J^{-1} \ll 1$, and on the average $\langle q \rangle \sim 0(k)$, thus $\langle q \rangle / \ell_M \sim N_J^{-1} \ll 1$. Then the first term in the integrand leads to $\log 1 = 0$. So, Eq. (51) becomes

$$\begin{aligned} I_2^{(1)}(z) &= \frac{2}{iv_{12}} \int_{-\infty}^{\infty} d\lambda \left(1 + \frac{z}{\lambda v_{12} - z}\right) \frac{-1}{q(q - 2\lambda)} \log \frac{\lambda^2 + k^2}{[(\lambda - q)^2 + k^2]} \\ &= 2 \left( \frac{z}{v_{12}} J_0 + J_1 \right) , \end{aligned} \tag{52}$$

where we introduce the integrated form $J_0$ and $J_1$ as

$$J_0 = \frac{1}{i} \int_{-\infty}^{\infty} d\lambda \, \frac{1}{\lambda v_{12} - z} \, \frac{1}{q(2\lambda - q)} \log \frac{\lambda^2 + k^2}{[(\lambda - q)^2 + k^2]} , \tag{53}$$

$$J_1 = \frac{1}{iv_{12}} \int_{-\infty}^{\infty} d\lambda \, \frac{1}{q(2\lambda - q)} \log \frac{\lambda^2 + k^2}{[(\lambda - q)^2 + k^2]} . \tag{54}$$

Similarly, from Eq. (45), we can write $\vec{I}^{(2)}(z)$ as

$$\vec{I}^{(2)}(z) = \frac{2}{i\pi} \int d\vec{\ell} \, \frac{1}{\vec{\ell} \cdot \vec{v}_{12} - z} \, \frac{\vec{\ell}\vec{\ell}}{(\ell^2 + k^2)[(\vec{\ell} - \vec{q})^2 + k^2]} , \tag{55}$$

and

$$\vec{I}^{(2)}(z) = I_1^{(2)}(z)\,(\hat{\ell}_x\hat{\ell}_x + \hat{\ell}_y\hat{\ell}_y) + I_2^{(2)}(z)\,\hat{\ell}_z\hat{\ell}_z\,. \tag{56}$$

Therefore,

$$\begin{aligned} I_1^{(2)}(z) &= \frac{2}{i\pi}\int_{-\infty}^{\infty} d\lambda\,\frac{1}{\lambda v_{12}-z}\int_0^{\ell_M} bdb \\ &\quad\times\int_0^{2\pi} d\phi\,\frac{b^2\sin^2\phi}{[b^2+\lambda^2+k^2][b^2+(\lambda-q)^2+k^2]} \\ &= \frac{1}{i}\int_{-\infty}^{\infty} d\lambda\,\frac{1}{\lambda v_{12}-z}\,\frac{\lambda^2+k^2}{q(q-2\lambda)}\log\frac{\lambda^2+k^2}{(\lambda-q)^2+k^2} \\ &\quad+\frac{1}{i}\int_{-\infty}^{\infty} d\lambda\,\frac{1}{\lambda v_{12}-z}\log\frac{\ell_M^2+k^2+(\lambda-q)^2}{(\lambda-q)^2+k^2} \\ &= -\left(k^2+\frac{z^2}{v_{12}^2}\right)J_0-\left(J_2+\frac{z}{v_{12}}J_1\right)+J_3\,. \end{aligned} \tag{57}$$

We introduce the integrated form $J_2$ and $J_3$ as

$$J_2 = \frac{1}{iv_{12}}\int_{-\infty}^{\infty} d\lambda\,\frac{\lambda}{q(2\lambda-q)}\log\frac{\lambda^2+k^2}{[(\lambda-q)^2+k^2]}\,, \tag{58}$$

$$J_3 = \frac{1}{i}\int_{-\infty}^{\infty} d\lambda\,\frac{1}{\lambda v_{12}-z}\log\frac{\mu^2+(\lambda-q)^2}{(\lambda-q)^2+k^2}\,, \tag{59}$$

where

$$\mu^2 = \ell_M^2 + k^2\,.$$

For the terms $I_2^{(2)}(z)$, we can write

$$\begin{aligned} I_2^{(2)}(z) &= \frac{2}{i\pi}\int_{-\infty}^{\infty} d\lambda\,\frac{1}{\lambda v_{12}-z}\int_0^{\ell_M} bdb \\ &\quad\times\int_0^{2\pi} d\phi\,\frac{\lambda^2}{[b^2+\lambda^2+k^2][b^2+k^2+(\lambda-q)^2]} \\ &= 2\,\frac{z^2}{v_{12}^2}J_0+2\,\frac{z}{v_{12}}J_1+2J_2\,. \end{aligned} \tag{60}$$

Now, we only need to calculate $J_0$, $J_1$, $J_2$, and $J_3$, respectively. We first calculate $J_3$ from Eq. (59). The integration over $\lambda$ can be performed by the method of residues. The integrand has a pole at $z/v_{12}$ and four branch points at $\lambda = q \pm ik$ and $\lambda = q \pm i\mu$. We now complete the real axis with a half-circle at infinity in the lower half-plane; we must, however avoid the two branch points by making a cut. This leads to the contour of Fig. 2.

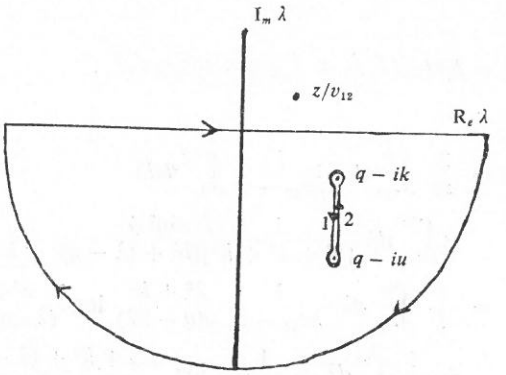


Fig. 2. The Contour for the Integration of $J_3$

As there is no pole within the contour, and as the large half-circle and the small circles around the branch points do not contribute, we finally obtain

$$J_3 = \frac{1}{i}\left\{\underbrace{\int_{q-i\mu}^{q-ik}}_{(1)} - \underbrace{\int_{q-i\mu}^{q-ik}}_{(2)}\right\} d\lambda \frac{1}{\lambda v_{12} - z} \log \frac{\mu^2 + (\lambda - q)^2}{(\lambda - q)^2 + k^2}$$
$$= \frac{2\pi}{v_{12}} \log \frac{z - \vec{q}\cdot\vec{v}_{12} + i\mu v_{12}}{z - \vec{q}\cdot\vec{v}_{12} + ik v_{12}} \approx \frac{2\pi}{v_{12}} \log \frac{z - \vec{q}\cdot\vec{v}_{12} + i\ell_M v_{12}}{z - \vec{q}\cdot\vec{v}_{12} + ik v_{12}}, \tag{61}$$

since

$$k/\ell_M \sim 0(N_J^{-1}) \ll 1, \ \mu = \sqrt{\ell_M^2 + k^2} \sim \ell_M .$$

Next, we calculate $J_0$ from Eq. (53). The integrand has poles at $z/v_{12}$ and $q/2$, and four branch points at $\lambda = \pm ik$ and $\lambda = q \pm ik$. This leads us to obtain

$$J_0 = \frac{2\pi}{q(2z - \vec{q}\cdot\vec{v}_{12})} \log \frac{z + ik v_{12}}{z - \vec{q}\cdot\vec{v}_{12} + ik v_{12}} . \tag{62}$$

Similarly, we can perform the same method to obtain

$$J_1 = \frac{\pi}{\vec{q}\cdot\vec{v}_{12}} \log \frac{\vec{q}\cdot\vec{v}_{12} + 2ik v_{12}}{-\vec{q}\cdot\vec{v}_{12} + 2ik v_{12}}, \tag{63}$$

$$J_2 = \frac{\pi}{2v_{12}} \log \frac{\vec{q}\cdot\vec{v}_{12} + 2ik v_{12}}{-\vec{q}\cdot\vec{v}_{12} + 2ik v_{12}} . \tag{64}$$

Therefore, from Eqs. (52)-(64), we can obtain the result of the integrals $\vec{I}^{(2)}$ and $\vec{I}^{(1)}$. Then the collision operator $\Lambda_q(z)$ (Eq. (44)) can be completely evaluated.

Among $J_0$, $J_1$, $J_2$, and $J_3$, only $J_3$ contains the term $\log \ell_M$ which is the asymptotically dominant contribution. The term $\vec{I}^{(2)} - \vec{q}\vec{I}^{(1)}$ in Eq. (44) can be written as

$$\vec{I}^{(2)} - \vec{q}\vec{I}^{(1)} = J_3(\hat{\ell}_x\hat{\ell}_x + \hat{\ell}_y\hat{\ell}_y) - \left[\left(k^2 + \frac{z^2}{v_{12}^2}\right)J_0 + \left(J_2 + \frac{z}{v_{12}}J_1\right)\right] (\hat{\ell}_x\hat{\ell}_x + \hat{\ell}_y\hat{\ell}_y) + I_2^{(2)}\hat{\ell}_z\hat{\ell}_z - \vec{q}\,I_2^{(1)}(z)\,\hat{\ell}_z \tag{65}$$

$$= \frac{2\pi}{v_{12}} \log \frac{z - \vec{q}\cdot\vec{v}_{12} + i\ell_M v_{12}}{z - \vec{q}\cdot\vec{v}_{12} + ikv_{12}} (\hat{I} - \hat{\ell}_z\hat{\ell}_z) + I(R),$$

where $I(R)$ represents all other terms except $J_3$ in Eq. (65), and $\hat{I}$ is the unit tensor. Therefore, from Eq. (44), we have

$$\Lambda_{\vec{q}}(z) = \frac{2\pi}{v_{12}} \gamma^2 \partial_{12} \cdot \log \frac{z - \vec{q}\cdot\vec{v}_{12} + i\ell_M v_{12}}{z - \vec{q}\cdot\vec{v}_{12} + ikv_{12}} \left(\frac{\hat{I}v_{12}^2 - \vec{v}_{12}\vec{v}_{12}}{v_{12}^2}\right)\cdot\partial_{12} + \bar{\Lambda}_{\vec{q}}(z), \tag{66}$$

where $\bar{\Lambda}_{\vec{q}}(z)$ represents the collision operator associated with $I(R)$ of Eq. (65) and the terms $-i[\partial(\vec{I}^{(2)} - \vec{q}\vec{I}^{(1)})/\partial z]$ of Eq. (44).

The inverse Laplace transform $\Lambda_{\vec{q}}(\tau)$ can be obtained from Eq. (66),

$$\Lambda_{\vec{q}}(\tau) = \frac{2\pi}{v_{12}} \gamma^2 \partial_{12} \cdot \int \frac{dz}{-2\pi} e^{-iz\tau} \log \frac{z - \vec{q}\cdot\vec{v}_{12} + i\ell_M v_{12}}{z - \vec{q}\cdot\vec{v}_{12} + ikv_{12}} \left(\frac{\hat{I}v_{12}^2 - \vec{v}_{12}\vec{v}_{12}}{v_{12}^2}\right)\cdot\partial_{12} + \int \frac{dz}{-2\pi} e^{-iz\tau} \bar{\Lambda}_{\vec{q}}(z)$$

$$= \frac{2\pi}{v_{12}} \gamma^2 \partial_{12} \cdot e^{-i\tau\vec{q}\cdot\vec{v}_{12}} \frac{1}{\tau} [e^{-kv_{12}\tau} - e^{-\ell_M v_{12}\tau}] \left(\frac{\hat{I}v_{12}^2 - \vec{v}_{12}\vec{v}_{12}}{v_{12}^2}\right)\cdot\partial_{12} + \int \frac{dz}{-2\pi} e^{-iz\tau} \bar{\Lambda}_{\vec{q}}(z). \tag{67}$$

The first terms in Eq. (67) are damped out faster than a time of the order of the crossing time $t_c = 1/kv_{12}$, because of the term $e^{-kv_{12}\tau}/\tau$. In $\bar{\Lambda}_{\vec{q}}(z)$, only $J_0$ has $z$-dependence. Therefore, only the time terms $e^{-kv_{12}\tau}$ and $e^{-iqv_{12}\tau}$ can appear in the second term of Eq. (67). Clearly, this term also decays on the time scale $t_c$. So $\Lambda_q(\tau)$ approaches zero as $\tau \gg t_c$. This is also true for $D(1, t)$, for practically any hypotheses we might make regarding the initial correlations ($D(1, t) \to 0$ as $\tau \gg t_c$).

For time $t \gg t_c$, the effect of memorizing the history of the system no longer appears, Eq. (46) will become the Markovian relation, and the time integral can be extended to infinity. Then it is easily shown that Eq. (46) becomes

$$\left[\frac{\partial}{\partial t} + \vec{v}_1 \cdot \vec{\nabla}_1 + \overline{\vec{K}_1} \cdot \frac{\partial}{\partial \vec{v}_1}\right] f(1)$$

$$= \frac{1}{8\pi^3} \int d\vec{x}_2\, d\vec{v}_2 \int d\vec{q}\, e^{i\vec{q}\cdot(\vec{x}_1 - \vec{x}_2)}\, \Lambda_q^{\rightarrow}(i0)\, f(1) f(2) + 0(\overline{\Lambda}_q^{\rightarrow}), \qquad (68)$$

where

$$\Lambda_q^{\rightarrow}(i0) = \lim_{z \to +i0} \int_0^{\infty} d\tau\, e^{iz\tau}\, \Lambda_q(\tau),$$

and $0(\overline{\Lambda}_q^{\rightarrow})$ denotes the integral associated with $\overline{\Lambda}_q^{\rightarrow}(z)$.

From Eq. (66), we obtain

$$\Lambda_q^{\rightarrow}(i0) = \frac{2\pi}{v_{12}} \gamma^2 \partial_{12} \cdot \log \frac{i\ell_M v_{12} - \vec{q} \cdot \vec{v}_{12}}{ik\, v_{12} - \vec{q} \cdot \vec{v}_{12}} \left(\frac{\hat{I} v_{12}^2 - \vec{v}_{12}\vec{v}_{12}}{v_{12}^2}\right) \cdot \partial_{12}$$

$$+ \overline{\Lambda}_q^{\rightarrow}(i0) \qquad (69)$$

$$\simeq \frac{2\pi}{v_{12}} \gamma^2 \partial_{12} \cdot \log \frac{\ell_M}{k} \left(\frac{\hat{I} v_{12}^2 - \vec{v}_{12}\vec{v}_{12}}{v_{12}^2}\right) \cdot \partial_{12} + \overline{\Lambda}_q^{\rightarrow}(i0).$$

Here we use the weak coupling approximation Eq. (49) and $\langle q \rangle \sim 0(k)$. So, Eq. (69) is independent of $\vec{q}$.

Finally, from Eqs. (68) and (69), the weakly coupled kinetic equation of nonuniform stellar systems takes on the form

$$\left[\frac{\partial}{\partial t} + \vec{v}_1 \cdot \vec{\nabla}_1 + \overline{\vec{K}_1} \cdot \frac{\partial}{\partial \vec{v}_1}\right] f(1)$$

$$= 4\pi^2 \gamma^2 \log \frac{\ell_M}{k} \int d\vec{x}_2\, d\vec{v}_2\, \delta(\vec{x}_1 - \vec{x}_2)\, \partial_{12} \cdot \left(\frac{\hat{I} v_{12}^2 - \vec{v}_{12}\vec{v}_{12}}{v_{12}^3}\right) \qquad (70)$$

$$\cdot \partial_{12} f(1) f(2) + 0(\overline{\Lambda}_p^{\rightarrow}).$$

## V. CONCLUSION

In the infinite homogeneous system, the kinetic equations generally have very simple interpretations in terms of the "golden rule", using dynamically shielded potentials, or in terms of the Boltzmann equation. But in the inhomogeneous system, the resulting equations are quite difficult to interpret,

even though we can show that the inhomogeneous system does have many of the characteristics of the homogeneous system[16].

A basic inadequacy of describing the stellar encounter in the infinite homogeneous medium is revealed by the fact that the scattering cross-section is divergent at long distances due to the long-range gravitational interaction. In our finite system, the linear dimension $L_J$ provides a natural cut-off to prevent the divergence and we replace the true gravitational potential by a screened potential $\varphi_{12}(r)$. On the other hand, at very short distances, where the interactions become very large, the divergence also shows up. We may set a limit of weak deflection at 90° to introduce a cut-off $L_{\min}$ (Eq. (49)). This approximation of ignoring the close collision effects is reasonable for the gravitational force.

In the collision operator $A_{12}$, the mean field $\overline{\vec{K}(\vec{x}_i)}$ was taken as uniform in the proximate encounter approximation[22] where the major contribution to the collision term comes from the proximate pair separation $r$ such that $r < r_0 \ll L_J$, and the classical description of encounters is shown to be valid in the limit $\log(\ell_M/k) \simeq \log N_J \sim \log N \gg 1$, where $N$ is the population of the system.

The methods which we used in calculating the collision operator $A_{12}$ were the familiar Fourier-Laplace transforms and contour integrations. These simple techniques provide us an easier way to handle those already complicated problems in the nonuniform system.

As discussed in section II, there are three relaxation stages in our system such that $t_c \ll t_r \ll t_h$ due to the weakly coupled nature of the system. Hence, to a good approximation the secular evolution stage can be ignored in our kinetic description of the intermediate kinetic stage which is characterized by a local Maxwellian velocity distribution. The theory of the slow secular evolution stage which is governed by the hydrodynamical equations remains a very interesting problem yet to be explored.

## REFERENCES

(1) Chandrasekhar, S., *Principles of Stellar Dynamics*, Univ. of Chicago Press. (1942).
(2) Jeans, J. H., *Monthly Notices Roy. Astron. Soc.* **76**, 70 (1915).
(3) Chandrasekhar, S., *Rev. Mod. Phys.* **15**, 1 (1943).

(4) Spitzer, L. and R. Harm, *Astrophys. J.* **127**, 544 (1958).
(5) Michie, R. W., *Monthly Notices Roy. Astron. Soc.* **125**, 127 (1963).
(6) Larson, R. B., *Monthly Notices Roy. Astron. Soc.* **147**, 323; **150**, 93 (1970).
(7) Aarseth, S., M. Henon and R. Wielen, *Astron. Astrophys.* **37**, 183 (1974).
(8) von Hoerner, S., *Astrophys. J.* **125**, 451 (1957).
(9) King, I., *Astron. J.* **67**, 471 (1962).
(10) King, I., *Astron. J.* **71**, 64 (1966).
(11) Cohen, R., L. Spitzer and P. Routly, *Phys. Rev.* **80**, 230 (1950).
(12) Prigogine, I. and G. Severne, *Physica* **32**, 1376 (1966).
(13) Ostriker, J. and A. Davidsen, *Astrophys. J.* **151**, 679 (1968).
(14) Haggerty, M. and G. Severne, *Physica* **51**, 461 (1971).
(15) Lerche, I., *Astrophys. J.* **166**, 207 (1971).
(16) Chappell, W., *J. Math. Phys.* **9**, 1921 (1968).
(17) Prigogine, I. and G. Severne, *Bull. Astron.* **3**, 273 (1968).
(18) Cohen, L. and A. Ahmad, *Astrophys. J.* **197**, 667 (1975).
(19) Lynden-Bell, D., *Monthly Notices Roy. Astron. Soc.* **136**, 101 (1967).
(20) Rostoker, N. and M. N. Rosenbluth, *Phys. Fluids* **3**, 1 (1960).
(21) Severne, G. and A. Kuszell, *Astrophys. Space Sci.* **32**, 447 (1975).
(22) Severne, G. and M. J. Haggerty, *Astrophys. Space Sci.* **45**, 287 (1976).
(23) Spitzer, L. Jr., *Physics of Fully Ionized Gases*, Interscience, New York, (1956).

# A MICROPROCESSOR-BASED CHINESE SYSTEM

YEONG-WEN HWANG

## ABSTRACT

A Chinese system is implemented on an Intel microprocessor demanding only a 12K bytes memory. Cost reduction by a decade is readily realizable. The GCS (Geometrical Component System) is especially suitable for the microprocessor due to the extremely small memory capacity needed and the avoidance of disk usage during Chinese I/O, so that low speed diskettes may be used.

The paper shows two models: one on MDS and one on SBC. The former is a stand-alone system having diskettes and an editor for Chinese data files. The latter is a terminal-equivalent slave system of extremely low cost for outputting Chinese as sent from another computer. The sent output is in component code form rather than in pattern form. Therefore the communication speed is greatly improved. The Chinese program is pre-stored in PROM and the PROM module may be plugged-in in both models. Samples of output on TV and printer are shown.

The rise of microprocessors offers a great opportunity for the efficient implementation of a Chinese system. Not only is a decade reduction of cost easily realized, but a significant step toward a universal means of Chinese data manipulation in all computers can now be taken. The cost reduction is an urgent requirement due to the expensiveness of equipments and CPU times of present Chinese systems.

The geometrical component system (hereafter abbreviated as GCS)[1] fits into this line very well. Two main reasons may be stated:

1. GCS needs less than 12K bytes memory space for the overall system, and this is easily provided by read only memory or RAM in a microprocessor.
2. GCS needs no disk operation at all in doing Chinese I/O. Therefore low speed diskettes which are commonly used in microprocessors play a satisfactory role in GCS.

A little more clarification of the above two reasons seems helpful. It is well known that a huge memory space is required if the patterns for tens

of thousands of existing Chinese characters are to be stored. The memory price is still too high, even with developments to be expected over the next few years, for such a storage to be economically feasible. Besides, hardware capacity and complexity are problems. GCS skips these patterns by composing them from simple components.

Secondly, cartridge disks, disk packs or similar devices, as they are designed to be accessed occasionally in file management, are overburdened by the irregularly frequent access (ranging from several times per character to once per several characters) if the character patterns are stored on disk. A disk pack used in such an input/output environment may wear out in just few months.

In this paper, the GCS Chinese system using an Intel 8080 microprocessor will be presented. It is implemented in two different models. One operates under Intel microprocessor developing system (MDS) and is a stand-alone Chinese system. Another is implemented in a "single board" type and is to be called by another computer.

The MDS model is as shown in Fig. 1. An Intel MDS-800 with dual diskette drivers is utilized. The implemented system has a 32K bytes RAM memory, but a 16K size may also be used. The diskettes are used for file management only.

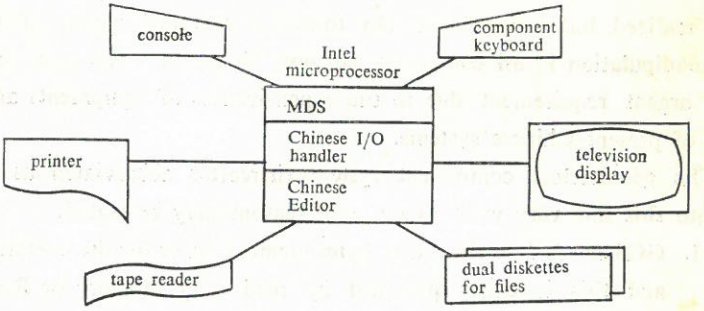


Fig. 1. System using Intel MDS.

The Chinese component keyboard[2] has 256 keys used for component keying-in. The printer is a K2000 impact dot-matrix type capable of making 5 copies. Character size is $16 \times 16$. A tape reader may be used to read in Chinese files or data.

## REFERENCES

(1) Hwang Y. W., "A New Component System with Geometrical Grammar and Improved Character Appearance", Proceedings of International Component Symposium, pp. 362-368, 1975, Taipei.

(2) Hwang Y. W., C. C. Hsieh, S. L.Liu and T. Chen, "Keyboard Design and Implementation of the Radical System", Proceedings of First International Symposium on Computers and Chinese I/O Systems, pp. 943-956, 1973, Taipei.

(3) Hwang Y. W. and H. Lee, "A Chinese File Management and Text Editor System on HP Computer", Chinese Language Computer Society Conference, Sept. 1977, Washington, D. C.

(4) Cheng L. H. and T. Y. Kiang, "A Chinese On-line Computer Operating System", Proceedings of National Computer Symposium, pp. 1-23, 1976, Taipei.

"So much science in the past has produced unpleasant results like pollution and nuclear bombs and germ warfare, that people are frightened of the next breakthrough."

D. J. R. BRUCKNER

"Peaceful use of atomic energy and real disarmament could make the earth the paradise it ought to be, if people would permit it."

ERNEST O. LAWRENCE

"Science inspires us with a feeling of hopefulness and infinite possibility."

I. I. RABI

# THE STABLE EQUILIBRIUM CONDITION FOR A CLOSED ISOMETRICAL SYSTEM OF COEXISTING LIQUID AND VAPOR PHASES SEPARATED BY A SPHERICAL INTERFACE

ARTHUR JING-MIN YANG

## I. INTRODUCTION

Surface phenomena have always been an attractive topic in the field of physical chemistry. Due to the surface effect, the thermodynamics for a small system is very different from that of large systems. In order to understand more about surface thermodynamics, a great deal of work has been done on the microscopic theory of interfaces[1~7].

In a previous paper[6] we provided a microscopic theory for a liquid-vapor interface. We showed that the three dimensional equilibrium density function, a function which extremizes the Helmholtz free energy of the system, satisfies a differential form of the Young-Laplace[8] equation for the pressure variation across a spherical interface. In that paper we only knew that the density function we obtained extremized the free energy; therefore, whether or not such a system is at a stable equilibrium was not determined.

In nucleation theory the Young-Laplace radius is considered as the critical nucleation size for a given temperature. This means that the equilibrium is unstable. In the absence of an external field, a two-phase system in stable equilibrium should also have a spherical interface, as dictated by spatial isotropy. Therefore, for the equilibrium between two phases separated by a spherical interface, the stability of the equilibrium is not clearly known.

In this paper we shall present a purely thermodynamic approach to discuss the stability of the equilibrium in a closed system at constant temperature and volume. The thermodynamic constraints of constant volume and number of particles are essential, because we know that the surface effect varies with the size of the system. The stability of the small system depends very much on the surface effect. We wish to derive the condition

for a stable equilibrium and also to study the dependence of the stability on the size of the system.

In section II, a general discussion of the equilibrium between liquid and vapor phases is introduced. We summarize thermal, mechanical, and diffusive equilibrium conditions by using three equations. In section III, we determine the stability of the system by considering the influence of small fluctuations on some physical properties of the system. The stable equilibrium condition is derived for a liquid drop in a vapor phase. In section IV, we use the physical constants of water at 293°K to do some calculations and estimate the influence of the system size on the stability of the equilibrium. The conclusion we obtain from the calculation is that whether a liquid drop of fixed radius $r$ is at a stable equilibrium or not is determined by the total amount of the vapor phase in the system. Or, in other words, the stability of this kind of equilibrium is dependent on the size of the system.

## II. GENERAL DISCUSSION OF THE EQUILIBRIUM BETWEEN VAPOR AND LIQUID PHASES

In a one component system containing two phases, a vapor phase and a liquid phase, there are three thermodynamic requirements for the existence of equilibrium. For thermal equilibrium the temperatures of two phases must be equal, and for diffusive equilibrium (or chemical equilibrium) the chemical potentials must be equal. The mechanical equilibrium in general can be described by the equation of Young and Laplace[8], i. e., for a spherical interface

$$P'' - P' = \frac{2\sigma}{r},$$

where $P''$ is the pressure of the inside phase and $P'$ is the pressure of the outside phase, $r$ is the radius of curvature, and $\sigma$ is the interfacial tension. For a general interface characterized by two radii of curvature, $r_1$ and $r_2$, at any point

$$P'' - P' = \sigma\left(\frac{1}{r_1} + \frac{1}{r_2}\right).$$

For a system which has coexisting vapor and liquid phases separated by a

spherical interface, these three thermodynamic equilibrium conditions can be summarized as follows

$T^G = T^L$, $\mu^G = \mu^K$, where $G$ indicates the gas phase and $L$ the liquid phase, and

$$P^L - P^G = \frac{2\sigma}{r}$$ (a liquid drop in a uniform vapor phase),

or

$$P^G - P^L = \frac{2\sigma}{r}$$ (a vapor bubble in a uniform liquid phase).

At a certain temperature $T$ below the critical temperature, the pressure-density isotherm of one component displays a two-phase region as shown in Fig. 1. The dashed lines are the extrapolation of the curve from the one phase region and represent the metastable or the supersaturated states. From the Maxwell relation we can derive the relation $dP = \rho d\mu$, where $\rho$ is the number density, and thus obtain a chemical potential density isotherm which also displays a two phase region (Fig. 2).

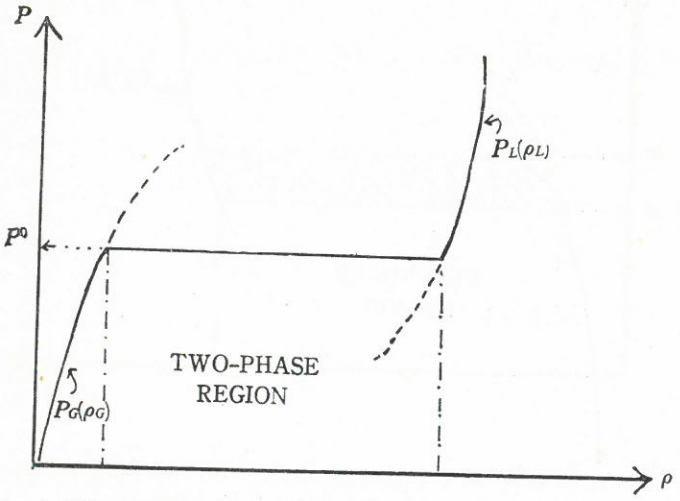


Fig. 1. The pressure density isotherm of a one component system at a temperature below critical temperature.

At $P$ equal to $P_0$, where $P_0$ is generally known as the normal vapor pressure of the component at temperature $T$, the equilibrium conditions are given by $T^G = T^L$, $\mu^G = \mu^L = \mu^0$, and $P^G = P^L = P^0$, where $\mu^0$ is generally called the coexisting chemical. This corresponds to a system which has a planar interface between the vapor and liquid phases. At some states with

chemical potentials other than $\mu^0$, there may exist an equilibrium between a stable state and a metastable state both states having the same chemical potential but different pressures. The pressure difference between these two states, $P^L - P^G$, is equal to the integral

$$\int_{\mu^0}^{\mu} (\rho_L - \rho_G) d\mu$$

and is shown as the shaded area in Fig. 2. In this situation the two phases can still reach a mechanical equilibrium as long as one phase, the high pressure one, assumes a spherical shape of radius $r$ such that $P'' - P' = 2\sigma/r$. Therefore the system which has two coexisting phases with the chemical $\mu$ greater than $\mu^0$ corresponds to a liquid drop in a uniform vapor phase, and the coexisting phases with the chemical potential $\mu$ less than $\mu^0$ corresponds to a vapor bubble in a uniform liquid phase[6].

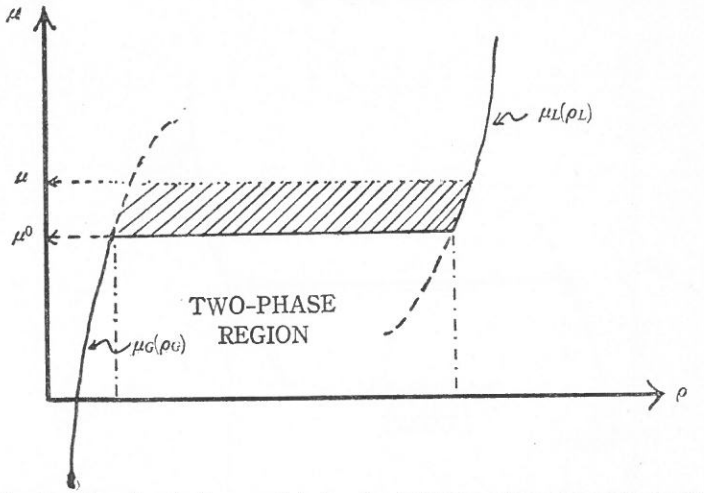


Fig. 2. The chemical potential density isotherm of a one component system at a temperature below critical temperature.

For the cases just discussed, although all three equilibrium conditions are satisfied, we still do not know whether or not such an equilibrium is stable. In most condensation theories the Young-Laplace radius $r$ for the mechanical equilibrium $P'' - P' = 2\sigma/r$ is considered as the critical radius for nucleation at a given temperature, and apparently the equilibrium is considered to be unstable. Suppose that a closed system of a liquid drop

of radius $r$ in a uniform vapor phase, at fixed volume $V$ and temperature $T$, is at this kind of unstable equilibrium. The liquid drop then starts growing, and due to the finite amount of the vapor phase in this volume, the growing process has to stop at some point where the liquid drop has a radius $r'$. At this stage the equilibrium is apparently stable. It seems that for a closed system at fixed volume and temperature, if there exists a Young Laplace radius $r$ which corresponds to an unstable equilibrium, then there is another Young-Laplace radius $r'$, $r' > r$, which corresponds to a stable equilibrium. This is what is actually observed in the Wilson cloud chamber. In the next section we discuss the stability of this kind of equilibrium and derive the condition of stable equilibrium for a closed system with fixed temperature and volume.

## III. THE STABLE EQUILIBRIUM CONDITION FOR A CLOSED SYSTEM AT FIXED TEMPERATURE AND VOLUME

To discuss the stability of the equilibrium we will first assume that the system has a small fluctuation which changes some physical properties of the system, and then examine the new values of these physical properties to determine whether, after this fluctuation, the system will tend to return to the equilibrium position or continue moving away from the equilibrium position. Since the system is at a fixed temperature, we only need to deal with variations of the chemical potential and the pressure of the system.

The closed system has a particle conservation condition which, in the system we are discussing, will be that

$$\rho'\left(V - \frac{4}{3}\pi r^3\right) + \rho''\frac{4}{3}\pi r^3 = N, \qquad \text{(III-1)}$$

where $\rho'$ is the density of the phase outside the sphere, and $\rho''$ is the density of the phase inside the sphere. If our system is a liquid drop in a uniform vapor phase, then $\rho'$ is $\rho_G$ and $\rho''$ is $\rho_L$, and at equilibrium $\rho_G$, $\rho_L$, and $r$ must satisfy the following equations

$$\rho_G\left(V - \frac{4}{3}\pi r^3\right) + \rho_L\frac{4}{3}\pi r^3 = N \qquad \text{(III-2)}$$

$$\mu_G(\rho_G) = \mu_L(\rho_L) \tag{III-3}$$

$$P_L(\rho_L) - P_G(\rho_G) = \frac{2\sigma}{r}\,. \tag{III-4}$$

Here $\mu_G(\rho_G)$ expresses the vapor chemical potential as a function of vapor density $\rho_G$ at constant temperature, and $\mu_L$ is the liquid chemical potential; $P_L(\rho_L)$, $P_G(\rho_G)$ are the liquid pressure and vapor pressure as functions of the liquid density and vapor density respectively.

In order to simplify the argument, it is useful to assume that while the system fluctuates one equilibrium condition, either the mechanical or the diffusive, is maintained and then discuss the variation of the other one. This is mathematically equivalent to solving a two-variable extremum problem by fixing one variable at a constant and looking at the partial derivative with respect to the other variable.

For the system of a liquid drop in a vapor phase we first assume the mechanical equilibrium is maintained and the number of particles in each phase fluctuates. We rewrite eq. (III-2) as

$$N_G + N_L = N$$

where $N_G = \rho_G(V - 4/3\,\pi r^3)$, $N_L = \rho_L(4/3\,\pi r^3)$, here $N_G$ and $N_L$ are the total number of particles in the vapor and liquid phases respectively. Evaluation of the differential yields

$$d\,N_G + d\,N_L = 0.$$

Thus

$$\rho_G(-4\pi r^2)dr + \left(V - \frac{4}{3}\,\pi r^3\right)d\rho_G = -\,\rho_L(4\,\pi r^2)dr\,. \tag{III-5}$$

The liquid has been considered as almost incompressible, and since $V \ll 4/3\,\pi r^3$, $4/3\,\pi r^3\,d\rho_L$ is negligibly small. Since the mechanical equilibrium is maintained, equation (III-4) enables us to write

$$d\left(P_L - P_G - \frac{2\sigma}{r}\right) = 0 \tag{III-6}$$

or, since $dP = \rho d\mu$, to obtain

$$\rho_L\,d\mu_L - \rho_G\,d\mu_G = d\left(\frac{2\sigma}{r}\right). \tag{III-7}*$$

If we substitute the relation

$$d\mu_G = \left(\frac{\partial \mu_G}{\partial \rho_G}\right)_T d\rho_G$$

into equation (III-7), we have

$$(\mu_L - \mu_G) = \frac{1}{\rho_L}\left\{(\rho_G - \rho_L)\frac{\partial \mu_G}{\partial \rho_G} d\rho_G + d\left(\frac{2\sigma}{r}\right)\right\}. \qquad \text{(III-8)}$$

We can see from equation (III-5) that

$$d\rho_G = \frac{4\pi r^2 (\rho_G - \rho_L)\, dr}{V - 4/3\pi r^3}. \qquad \text{(III-9)}$$

Thus if we assume that $\sigma$ is practically constant as long as the temperature of the system is not changed, we have

$$d(\mu_L - \mu_G) = \frac{1}{\rho_L}\left\{\frac{(\rho_G - \rho_L)\frac{\partial \mu_G}{\partial \rho_G}(\rho_G - \rho_L) 4\pi r^2\, dr}{V - 4/3\pi r^3} - \frac{2\sigma}{r^2} dr\right\} \qquad \text{(III-10)}$$

or, since $dN_L = \rho_L (4\pi r^2)\, dr$, we obtain

$$d(\mu_L - \mu_G) = \frac{1}{\rho_L (4\pi r^2)}\left\{\frac{(\rho_G - \rho_L)^2 \frac{\partial \mu_G}{\partial \rho_G}(4\pi r^2)}{V - 4/3\pi r^3} - \frac{2\sigma}{r^2}\right\} dN_L. \qquad \text{(III-1)}$$

We define the quantity $M$ by

$$M = (\rho_G - \rho_L)^2 \frac{4\pi r^2 \frac{\partial \mu_G}{\partial \rho_G}}{(V - 4/3\pi r^3)} - \frac{2\sigma}{r^2}. \qquad \text{(III-12)}$$

Since $\rho_L(4\pi r^2)$ is positive and if $M$ is greater than zero, then

$$\frac{d(\mu_L - \mu_G)}{dN_L} > 0,$$

which implies that if the fluctuation increases the number of particles of the liquid phase, i. e. $dN_L > 0$, the liquid phase will then have a higher chemical potential than the vapor phase, and thus the system tends to go back to the equilibrium through the diffusive process, i. e. the equilibrium is a stable one. By the same argument we see that when $M$ is negative,

$$\frac{d(\mu_L - \mu_G)}{dN_L} < 0,$$

* Due to the high incompressibility of the liquid $d\mu_L$ is not negligible even though $d\rho_L$ is negligibly small.

and the equilibrium is then obviously an unstable one.

If we assume that the diffusive equilibrium is maintained and look at the volume fluctuation, the argument is quite similar. Since the total volume is a constant we have

$$dV_L = -dV_G = 4\pi r^2 dr \tag{III-13}$$

where $V_L = 4/3\pi r^3$ and $V_G = V - 4/3\pi r^2$ are the volumes of the vapor and liquid phases respectively. While the volume fluctuates, the diffusive equilibrium is maintained and therefore equation (III-3) gives

$$d\mu_L = d\mu_G.$$

Since we know $dP = \rho d\mu$, we obtain

$$\begin{aligned} d\left(P_L - P_G - \frac{2\sigma}{r}\right) &= (\rho_L - \rho_G)d\mu - d\left(\frac{2\sigma}{r}\right) \\ &= (\rho_L - \rho_G)\frac{\partial \mu_G}{\partial \rho_G} d\rho_G - d\left(\frac{2\sigma}{r}\right). \end{aligned} \tag{III-14}$$

The particle conservation condition still holds, and combining equation (III-14) with equation (III-5), yields

$$d\left(P_L - P_G - \frac{2\sigma}{r}\right) = (\rho_L - \rho_G)\frac{\partial \mu_G}{\partial \rho_G}\frac{4\pi r^2(\rho_G - \rho_L)}{(V - 4/3\pi r^3)} dr + \frac{2\sigma}{r^2} dr. \tag{III-15}$$

Substituting (III-13) into equation (III-15) we have

$$\begin{aligned} d\left(P_L - P_G - \frac{2\sigma}{r}\right) &= -\frac{1}{4\pi r^2}\left\{(\rho_L - \rho_G)^2 \frac{4\pi r^2 \frac{\partial \mu_G}{\partial \rho_G}}{V - 4/3\pi r^3} - \frac{2\sigma}{r^2}\right\} dV_L \\ &= \frac{-1}{4\pi r^2} M\, dV_L \end{aligned} \tag{III-16}$$

where $M$ is defined by equation (III-12).

At equilibrium $P_L - P_G = 2\sigma/r$; if the fluctuation makes $d(P_L - P_G - 2\sigma/r) > 0$, indicating that after the fluctuation $P_L - P_G > 2\sigma/r$, the liquid phase is going to expand and the vapor phase contracts. Thus we can see from equation (III-16) that the equilibrium will be stable if $M$ is positive and unstable if $M$ is negative. Just as we expected, the two different paths give the same result.

We have obtained the condition for the system to be at a stable equilibrium. One point we have to emphasize here is that our treatment is only

for a system at fixed volume and temperature. If the system is open or isobaric, equation (III-1) is no longer valid and therefore the argument will be totally different. In the next section we use the physical constants of water to determine the influence of the size of the system on the stability of the system.

## IV. THE INFLUENCE OF SYSTEM SIZE ON THE STABILITY OF THE SYSTEM

We use the physical constants of water at 293°K to do the calculation. In doing the calculation we adopt three reasonable approximations: (1) We treat the vapor as an ideal gas; (2) we assume $\sigma$ to be independent of the radius $r$; (3) we neglect $\rho_G$ relative to $\rho_L$. The following physical constants of water are those needed for the calculation.

| | | | |
|---|---|---|---|
| $\sigma$ | $7.275 \times 10^{-2}$ | N/m | |
| $\rho_L$ | 55506 | mole/m$^3$ | |
| $\rho_G^0$ | 0.95915 | mole/m$^3$ | |
| $P_G^0$ | 17.535 | torr | "normal vapor pressure" |

To calculate the vapor pressure of a liquid drop of radius $r$ we use the Kelvin equation[9]

$$\ln\left(\frac{P}{P^0}\right) = \frac{2\sigma}{RT\rho_L r}, \tag{IV-1}$$

or, since the vapor is ideal,

$$\ln\left(\frac{\rho_G}{\rho_G^0}\right) = \frac{2\sigma}{RT\rho_L r}. \tag{IV-2}$$

The results are shown in Table 1.

Table I. The minimum volume, $V_c$, of the equilibrium vapor phase necessary to make the liquid drop of radius $r$ become unstable.

| $r$, Å | $10^2$ Å | $10^3$ Å | $10^4$ Å | $10^5$ Å | $10^6$ Å |
|---|---|---|---|---|---|
| $\rho_G$, mole/m$^3$ | 1.0681 | 0.96952 | 0.96018 | 0.95825 | 0.9516 |
| $V_c$, cm$^3$ | $2.02\times10^{-12}$ | $2.23\times10^{-8}$ | $2.26\times10^{-4}$ | 2.32 | $2.33\times10^{4}$ |

For the ideal gas, we know

$$dP_G = RT\, d\rho_G.$$

This, combined with the relation

$$dP_G = \rho_G\, d\mu_G,$$

gives

$$\left(\frac{\partial \mu_G}{\partial \rho_G}\right)_T = \frac{RT}{\rho_G}. \tag{IV-3}$$

Therefore $M$ can be expressed as

$$M = \rho_L^2 \frac{4\pi r^2}{(V - 4/3\pi r^3)} \cdot \frac{RT}{\rho_G} - \frac{2\sigma}{r^2}. \tag{IV-4}$$

For a liquid drop in equilibrium with a vapor phase of density $\rho_G$, we can see from equation (IV-4) that the stability of the equilibrium depends on the total volume. If we keep the vapor density at constant $\rho_G$, this will also fix the equilibrium radius $r$, and increase the total amount of the vapor phase, then it is very obvious that this process will decrease $M$ and may change the equilibrium from a stable one to an unstable one. For a liquid drop of radius $r$, we define the critical volume, $V_C$, as the minimum volume of the equilibrium vapor phase necessary to make the equilibrium become unstable, or make $M$ negative. We calculate the $V_C$'s for a liquid drop at different radii and show the results in Table 1.

We can use the data shown in Table 1 to discuss the stability of a system. For an appreciable supersaturation, the corresponding Young-Laplace radius $r$ is of the order $10^2$ Å to $10^4$ Å. Therefore, if the system is of an ordinary size, from a few cubic centimeters to a few liters, the equilibrium is apparently unstable. After growing in a closed system, the liquid drop will have a radius which is greater than or approximately equal to $10^6$ Å. Thus the equilibrium vapor pressure is almost exactly $P_G^0$, and from data shown in Table 1, it is clear that the volume of an ordinary size system is less than $V_C$, and the system is at stable equilibrium.

## V. DISCUSSION

In the preceding sections we have discussed in detail the stability of the equilibrium between a liquid drop and a vapor phase. We concluded

that a Young-Laplace radius can also be a stable equilibrium radius if the phase outside the sphere is sufficiently small.

In this paper we have only discussed the stability for a closed system at constant temperature and volume. For these constraints, a stable or metastable equilibrium corresponds to a local minimum of the Helmholtz free energy, and an unstable equilibrium corresponds to a local maximum. In a subsequent paper we will explain the fact that for a definite Young-Laplace radius, $r$, the stability is dependent on the size of the system by studying the influence of the surface free energy on the total Helmholtz free energy. We also will discuss the stability of a system at constant temperature and pressure, or at constant temperature and chemical potential. We hope that from this approach we can obtain some understanding, in the field of statistical thermodynamics, of the canonical ensemble and grand canonical ensemble of liquid-vapor coexisting systems.

## REFERENCES

(1) van der Waals, J. D., *Z. Phys. Chem.* **13**, 657 (1894).
(2) Cahn, J. W. and J. E. Hilliard, *J. Chem. Phys.*, **28**, 258 (1958).
(3) Rice, O. K., *J. Phys. Chem.*, **64**, 976 (1960).
(4) Buff, F. P., R. A. Loyett and F. H. Stillinger, *Phys. Rev. Letters*, **15**, 621 (1965).
(5) Widom, B., *J. Chem. Phys.*, **50**, 3219 (1969).
(6) Yang, A. J. M., P. D. Fleming and J. H. Gibbs, *J. Chem. Phys.*, **64**, 3732, (1976).
(7) Fleming, P. D., A. J. M. Yang and J. H. Gibbs, *J. Chem. Phys.*, **65**, 7, (1976).
(8) The usual reference is to J. W. Gibbs, Scientific Papers. (Dover, New York, 1961) Vol. 1, p. 229, eq. 500.
(9) Moore, *Physical Chemistry*, 4th edition, pp. 481-482.

"Look around the world. Contemplate the whole and every part of it. You will find it to be nothing but one great machine, subdivided into an infinite number of lesser machines."

DAVID HUME

"The big question men must face up to is: How many people can the Earth support, and at what standard of living?"

IRVING BENGELSDORF

"Life is not complex. We are complex. Life is simple and the simple thing is the right thing."

OSCAR WILDE

# THE EFFECT OF EXTRACTION TEMPERATURE AND ANTIOXIDANT ON THE FLAVOR OF SOYMILK AND THE EFFECT OF FLAVORINGS ON THE ACCEPTABILITY OF SOYMILK PUDDING

YUH-RONG CHOU

## ABSTRACT

Soymilks were prepared by three different methods which differ in the temperature of extraction and addition of antioxidant. Extraction at 60°C with added ascorbic acid as antioxidant produced a better soymilk than room temperature or 80°C extraction without added ascorbic acid. The yield of soymilk decreased with increasing extraction temperature. When soymilk was used for puddings with flavorings, the beany flavor was very well covered and the products were highly acceptable. Among them, chocolate gave the best flavor with soymilk. As soybean is a cheap source of protein in many Asian countries where cow's milk or meat is very expensive, it appears that soybean products have a great potential as substitutes for animal protein.

## INTRODUCTION

The purpose of this study was to investigate the effect of temperature and antioxidant upon the quality of soymilk, and to find out acceptable flavorings for puddings made with soymilk.

Soybean and soybean products have played an important role for many years as a source of protein in the diet of millions of people in Asia. They are more important in the nutrition of these people than are wheat in the U. S. or rye in Germany[1]. Soybean products are good sources not only of protein, but of fat rich in linoleic acid, calcium, iron, thiamine and riboflavin, though some of these nutrients are reduced or increased during processing[2]. Miller *et al.*[3] indicate a low retention of thiamine (18%) when

soybeans are made into soybean curd and preserved in water by the usual commercial process. They also indicate that the water drained from the soybean curd contains more vitamins than the soybean curd. Jackson[4] prepared soybean cheese using soybeans, skim milk powder, rennet, and lactic starter cultures. He attempted to reduce the beany flavor but was unsuccessful.

Soymilk prepared from soaked beans by a water extraction process has been the conventional method practiced in the Orient for centuries. This type of soymilk is usually too rancid in flavor for acceptance as a product in most countries[5]. The rapid formation of rancid flavors occurred almost instantly during the grinding of soybeans with water and was shown to be due to oxidation of polyunsaturated fats catalyzed by lipoxidases[6].

A high temperature, rapid hydration grinding process inactivated the lipoxidase system and produced a nearly bland soymilk. Wilkens *et al.*[6] reported that an acceptable bland soymilk was produced by grinding at temperatures between 80° and 100°C and maintaining the temperature for 10 minutes to completely inactivate the lipoxidase enzyme. Lower temperatures in the range of 60 to 80°C can be used, if sufficient antioxidants are added to the water.

Although high extraction temperatures were shown to be desirable in producing a relatively rancid-free milk, the use of temperatures above 85°C for extraction would also result in substantial losses in yields[7]. The decrease in volume at high temperatures is caused by difficulties in filtering the slurry. This is due to the formation of a gel that formed an impervious layer on the filter and prevented efficient filtration[8]. Wilkens *et al.*[6] reported that soaking at higher temperatures drastically reduced the yield of soymilk. According to these workers, although maximum solids are extracted at 50 to 70°C, with a decrease in solids at higher temperatures, a minimum temperature of 80°C should be employed at the initiation of grinding to prevent off-flavor development.

It is especially interesting that the protein from the insoluble residue, discarded in the water extract method for making soymilk, is actually superior in its protein efficiency ratio to the milk itself[9]. The protein residue may be dried for utilization after adequate heat treatment as a cereal-like product[5].

The flavor of soymilk is greatly enhanced by adding some flavorings.

Steinkraus *et al.*[10] reported the development of flavored soymilk and soy/coconut milk with flavors acceptable to children in the Philippines. They used various amounts of sucrose, vanilla, coconut milk and chocolate, and the products were highly acceptable. In Hong Kong, Vitasoy, produced by the Hong Kong Soya Bean Product Co., Ltd., has been the largest single seller in the local soft drink market when such internationally known brands as Coca Cola, Pepsi Cola, and Seven Up were competing with it[11].

Soymilk could also be useful as a low-methinoine substitute for cow's milk in the dietary therapy of metabolic disorders such as homocystinuria and cystinosis[12].

## MATERIALS AND METHODS

### A. Preparation of Soymilk

Tainung No. 4 soybeans were used throughout the experiment.

**Ingredients:**

| | |
|---|---|
| Soaked soybean | 100 g. |
| Blending water | 400 g. |
| Product A | 0.15% sodium bicarbonate solution (24°C)* |
| Product B | 0.15% sodium bicarbonate solution (80°C) |
| Product C | 0.15% sodium bicarbonate and 0.1% ascorbic acid solution (60°C) |
| Sugar | 40 g. |
| Salt | 3 g. |
| Vanilla | 0.5 g. |

*Steinkraus *et al.*[10] reported that the taste panel was unanimous in preferring soymilks containing 0.15% $NaHCO_3$ to those containing no sodium bicarbonate.

**Equipment:**

1 Quart Tatung blender
1 1. Volumetric flask
500 ml. Graduate cylinder
3 450 ml. Beakers
3 Rubber spatulas
1 Thermometer

3 Medium size aluminum sauce pans
3 Medium size pyrex bowls
1 Large wire strainer
1 Small wire strainer
1 Cheese cloth
1 Toledo balance
1 Top-loading Mettler balance

**Procedures:**

1. Dry soybeans were carefully washed and sorted to remove dirt and damaged beans.
2. The soybeans were soaked for 10 hours in 3 times their weight of 0.1% sodium hydroxide solution.**
3. The soybeans were drained and rinsed.
4. The soybeans were blended with variable blending solutions for 3 minutes at high speed.
5. The soybean slurry was filtered through three folds of cheese cloth.
6. Sugar and salt were added.
7. The extract was heated carefully with stirring at medium heat until the boiling point was reached (10 minutes).
8. Soymilk was cooled to room temperature and vanilla was added.
9. The yields of milks were weighed and the pH of each was measured.

**Steinkraus *et al.*[10] reported that the taste panel was unanimous in preferring soymilks prepared from Taichung soybeans soaked in dilute alkali (0.1% NaOH) to those soaked in water.

## B. Preparation of Pudding

Four different kinds of commercially prepared pudding mixes (Jello) were used for the preparation of pudding: vanilla, lemon, butterscotch and chocolate. Soymilk was prepared fresh for each trial by the method used for product C in previous experiment.

**Ingredients:**

Pudding mix 95 g. (1 package)
A Vanilla
B Lemon

C Butterscotch

D Chocolate

Soymilk 488 g. (2 cups)

**Equipment:**

4 600 ml. Beakers

2 Rubber spatulas

2 Glass double boilers

16 Custard cups

1 Top-loading Mettler balance

**Procedures:**

Milk was slowly added to pudding mix in a glass double boiler and mixed thoroughly. The mixture was cooked with stirring until thickened, and then covered and cooked for 15 minutes. Pudding was poured into custard cups and was allowed to chill in the refrigerator until firm.

## C. Scoring

The three laboratory prepared products and one kind of commercially prepared product (Pu Shih Soymilk) were compared with respect to aroma, taste, color, and texture by four trained taste panels. The panels were instructed as to the desirable qualities of the products and the method of scoring. The score cards were as follows:

### 1. QUALITY SCORE

Basis of Scoring: Date_____

Name_____

Aroma—no beany odor

Taste—no bitter taste of beans

Color—creamy white

Texture—homogeneous mixture with no residues

Directions:

Score each product according to the following scale:

1 excellent

2 good

3 fair
4 poor
5 unacceptable

| product | aroma | taste | color* | texture* |
|---|---|---|---|---|
| A | | | | |
| B | | | | |
| C | | | | |
| D | | | | |

Comments:
*For the scoring of puddings, color and texture were omitted.

## 2. PREFERENCE SCORE

Directions:

Arrange the products in order of your preference, labeling the product you like the most as 1 and the one you like the least as 4.

| product | preference |
|---|---|
| A | |
| B | |
| C | |
| D | |

## RESULTS AND DISCUSSION

**Test of the Flavor of Soymilk**

The results of quality scores are reported in Table 1.

The result of the scoring was about the same as the experimenter had expected. As shown in Table 1, product C consistently received the highest score, and product A received the lowest score among laboratory prepared soymilks. All laboratory prepared soymilks were preferred to commercially prepared product. The commercial product was unacceptable because of its

Table 1. Average scores* of judges on soymilk

| Trial / Product | Aroma | | Taste | | Color | | Texture | | Overall Score | |
|---|---|---|---|---|---|---|---|---|---|---|
| | I | II | I | II | I | II | I | II | I | II |
| A** | 3.4 | 3.5 | 3.8 | 2.8 | 3.0 | 3.0 | 3.4 | 1.5 | 3.4 | 2.8 |
| B | 3.4 | 3.3 | 3.0 | 2.2 | 2.3 | 3.0 | 3.0 | 1.5 | 2.9 | 2.5 |
| C | 2.3 | 1.8 | 4.0 | 2.0 | 1.4 | 2.8 | 3.0 | 1.5 | 2.7 | 1.9 |
| D | 4.0 | 4.0 | 4.0 | 4.5 | 4.8 | 5.0 | 4.8 | 4.8 | 3.9 | 4.5 |

* Average of 4 judges.
** A—Room temperature sodium bicarbonate solution extraction.
B—80°C sodium bicarbonate solution extraction.
C—60°C sodium bicarbonate, with added ascorbic acid, extraction.
D—Commercial product.

color and texture.

Ascorbic acid was chosen as antioxidant for this study so that the product can also be an ascorbic acid supplier.

A preference evaluation showed that product B and C were preferred. (Table 2)

Table 2. Ranking of laboratory prepared soymilk and commercially prepared soymilk

| Product | Judges | | | |
|---|---|---|---|---|
| | I | II | III | IV |
| A | 4 | 3 | 3 | 3 |
| B | 1 | 2 | 2 | 1 |
| C | 3 | 1 | 1 | 2 |
| D | 2 | 4 | 4 | 4 |

Table 3. Some organoleptic and chemical characteristics of soymilk

| Product | Color | Flavor | Texture | pH |
|---|---|---|---|---|
| A | yellowishwhite | painty | homogeneous | 8.39 |
| B | yellowishwhite | eggy | homogeneous | 8.35 |
| C | creamy white | little aroma | homogeneous | 7.62* |
| D | reddish brown | beany | residues | 6.39 |

* The lower pH of C was due to the added ascorbic acid. pH of whole cow's milk was 6.66.

A study was conducted to test some organoleptic and chemical characteristics of soymilk. The results of this study are shown in Table 3.

The yields of soymilk were weighed to see the effect of extraction temperature on the yield of soymilk. (Table 4)

Table 4. Yields of soymilks

| Product | A | B | C |
|---|---|---|---|
| Yield (g) | 439 | 391 | 411 |

The yield of milk decreased with increasing extraction temperature as expected.

**Test of the Acceptability of Soymilk Pudding**

To test the acceptability of soymilk pudding with different kinds of flavorings, quality and preference cards were used, the results of which are recorded in Tables 5 & 6.

Table 5. Average* scores of judges on soymilk puddings

| Trial / Product | Aroma | | Taste | | Overall Score | |
|---|---|---|---|---|---|---|
| | I | II | I | II | I | II |
| A** | 2.0 | 3.8 | 3.0 | 3.3 | 2.5 | 3.5 |
| B | 3.3 | 4.0 | 4.5 | 3.8 | 3.9 | 3.9 |
| C | 1.8 | 2.3 | 2.3 | 1.8 | 1.9 | 1.9 |
| D | 1.3 | 1.8 | 2.0 | 1.8 | 1.6 | 1.8 |

* Average of four judges.
** A—Vanilla. B—Lemon. C—Butterscotch. D—Chocolate.

Table 6. Ranking of soymilk pudding

| Products | Judges | | | |
|---|---|---|---|---|
| | I | II | III | IV |
| A | 4 | 3 | 3 | 3 |
| B | 3 | 4 | 4 | 4 |
| C | 2 | 2 | 1 | 1 |
| D | 1 | 1 | 2 | 2 |

As can be seen from Table 6, almost all products were evaluated as acceptable except product B (lemon). Two panel members stated that the beany flavor was almost completely covered in product D (chocolate). One of the panel members suggested adding some sugar to product D. Judges scored the product A (vanilla) as very beany. As can be seen from Table 6, products C and D were preferred over products A and B.

## REFERENCES


(1) Bailey, L. H., R. G. Capen, and J. A. LeClere, The composition and characteristics of soybeans, soybean flour, and soybean bread, *Cereal Chem.* **12**, 441(1935).

(2) Muto, S., E. Takahashi, M. Hara, and Y. Kenuma, Soybean products as protein sources for weanling infants. *J. Am. Dietet. Association*, **43**, 451-456 (1963).

(3) Miller, C. D., H. Denning, and A. Bauer, Retention of Nutrients in Commercially prepared Soybean Curd, *J. Am. Dietetics Association* (1952).

(4) Schroder, P. D. J., and H. Jackson, Preparation and Evaluation of Soybean Curd with Reduced Beany Flavor, *J. Food Science*, **37**, 450 (1972).

(5) Wilkens, W. F., and L. R. Hackle, Effect of processing conditions on the composition of soymilk, *Cereal Chem*, **4b** (4), 391-399 (1969).

(6) Wilkens, W. F., L. R. Mattick, and D. B. Hand, Effect of processing method on oxidative off-flavors of soybean milk, *Food Technol.* **21**, 1630-1633 (1969).

(7) Lo, W. Y., K. H. Steinkraus, D. B. Hand, L. B. Hackler, and E. F. Wilkens, Yield of extracted solids in soymilk as affected by temperature of water of various pre-treatments of beans, *Food Technol.* **22**, 1322-1324 (1968).

(8) Lo, W. Y., K. H. Steinkraus, D. B. Hand, L. B. Hackler, and W. F. Wilkens, Soaking soybeans before extraction as it affects chemical composition and yield of soymilk, *Food Technol.* **22**, 1188-1190 (1968).

(9) Hand, D. B., K. H. Steinkraus, J. P. Van Buren, L. R. Hackler, I. El Rawi, and H. R. Pallensen, Pilot plant studies on soymilk, *Food Technol.* **18**, 1963-1965 (1964).

(10) Steinkraus, K. H., L. T. David, L. J. Ramos, and J. Bason, Development of flavored soymilks and soy/coconut milk for the Philippine market, *Philippine Agriculturist* **52**(5), 268-296 (1968).

(11) Lo, K. S., Pioneering soymilk in Southeast Asia, *Soybean Digest* **24**(7), 18-20 (1974).

(12) Shih, V. E., Soybean milk, *J. Am. Dietet. Association*, **57**(6), 520-521 (1970).

"I didn't learn anything because the teacher always answered my questions."

AMERICAN STUDENT

"...because I had expected him (Don Juan) to hand out all the information. If he had done so, he said, I would never have learned."

CASTANEDA

# 輔仁學報

第十二號

發行者　私立輔仁大學

出版者　私立輔仁大學理學院
臺北縣新莊鎮中正路五一〇號

承印者　大進印刷有限公司
臺北市西藏路二五一巷八號
電話：3031449・3039249

中華民國六十七年十二月三十日出版